

Tracing of *her5* progeny in zebrafish transgenics reveals the dynamics of midbrain-hindbrain neurogenesis and maintenance

Alexandra Tallafu  and Laure Bally-Cuif*

Zebrafish Neurogenetics Junior Research Group, Institute of Virology, Technical University-Munich, Trogerstrasse 4b, D-81675 Munich, Germany

GSF-National Research Center for Environment and Health, Institute of Developmental Genetics, Ingolstaedter Landstrasse 1, D-85764 Neuherberg, Germany

*Author for correspondence (e-mail: bally@gsf.de)

Accepted 30 May 2003

SUMMARY

The midbrain-hindbrain domain (MH) of the vertebrate embryonic neural tube develops in response to the isthmic organizer (IsO), located at the midbrain-hindbrain boundary (MHB). MH derivatives are largely missing in mutants affected in IsO activity; however, the potentialities and fate of MH precursors in these conditions have not been directly determined. To follow the dynamics of MH maintenance in vivo, we used artificial chromosome transgenesis in zebrafish to construct lines where *egfp* transcription is driven by the complete set of regulatory elements of *her5*, the first known gene expressed in the MH area. In these lines, *egfp* transcription faithfully recapitulates *her5* expression from its induction phase onwards. Using the stability of GFP protein as lineage tracer, we first demonstrate that *her5* expression at gastrulation is a selective marker of MH precursor fate. By comparing GFP protein and *her5* transcription, we further reveal the spatiotemporal dynamics of *her5* expression that conditions neurogenesis progression towards the MHB

over time. Finally, we trace the molecular identity of GFP-positive cells in the *acerebellar* (*ace*) and *no-isthmus* (*noi*) mutant backgrounds to analyze directly *fgf8* and *pax2.1* mutant gene activities for their ultimate effect on cell fate. We demonstrate that most MH precursors are maintained in both mutants but express abnormal identities, in a manner that strikingly differs between the *ace* and *noi* contexts. Our observations directly support a role for Fgf8 in protecting anterior tectal and metencephalic precursors from acquiring anterior identities, while Pax2.1 controls the choice of MH identity as a whole. Together, our results suggest a model where an ordered MH pro-domain is identified at gastrulation, and where cell identity choices within this domain are subsequently differentially controlled by Fgf8 and Pax2.1 functions.

Key words: *her5*, Midbrain-hindbrain, Midbrain-hindbrain boundary, Zebrafish, *acerebellar*, *no-isthmus*, ET-cloning, Transgenesis

INTRODUCTION

Building of the vertebrate embryonic brain is a progressive process that involves a number of consecutive steps controlling patterning and neurogenesis events. Both processes respond to phases of induction and refinement, during which the positional identity and differentiation status of neural cells are specified, maintained or modified in a dynamically controlled manner. Unraveling the dynamics of neural patterning and neurogenesis are crucial steps in our understanding of brain development. Indeed, it will highlight the potentialities of given neural territories, thus revealing how their fate and differentiation are progressively restricted in vivo.

The midbrain-hindbrain (MH) domain of the embryonic neural tube displays extensive plasticity linked to specific ontogenic properties that make it an important model to study developmental dynamics (Martinez, 2001; Rhinn and Brand, 2001; Wurst and Bally-Cuif, 2001). The MH can be morphologically identified at early somitogenesis stages as

comprising the mesencephalic vesicle and the first rhombencephalic vesicle (or metencephalon) (Fig. 1); the latter – also called ‘rhombomere A’ in the chicken embryo (Vaage, 1969) – will later subdivide into rhombomeres (r) 1 and 2. Detailed fate map analyses in avian embryos demonstrated that the mesencephalon generates all midbrain structures, i.e. essentially an alar visual center, the tectum and a basal tegmentum, containing cranial motoneuron III (Marin and Puelles, 1994; Martinez and Alvarado-Mallart, 1989). In addition, the caudal third of the alar mesencephalic domain contributes to the dorsomedial part of the cerebellar plate (Hallonet and Le Douarin, 1990; Hallonet et al., 1993; Martinez and Alvarado-Mallart, 1989), while the alar domain of r1 will give rise to remaining, lateral cerebellar structures (Wingate and Hatten, 1999) (Fig. 1). Finally, the basal r1 territory will generate the pons, of which a prominent output is cranial motoneuron IV. These distinct fates are prefigured by molecular gradients in the expression of MH genes such as *engrailed-2/3* or *ephrins* (Martinez, 2001; Rhinn and Brand,

2001; Wurst and Bally-Cuif, 2001). MH structures, although physically and functionally distinct, develop in a concerted fashion. Their growth and patterning is dependent upon and coordinated by an organizing center [the ‘isthmus organizer’ (IsO) or ‘isthmus’] located at the midbrain-hindbrain boundary (MHB) (Martinez, 2001; Rhinn and Brand, 2001; Wurst and

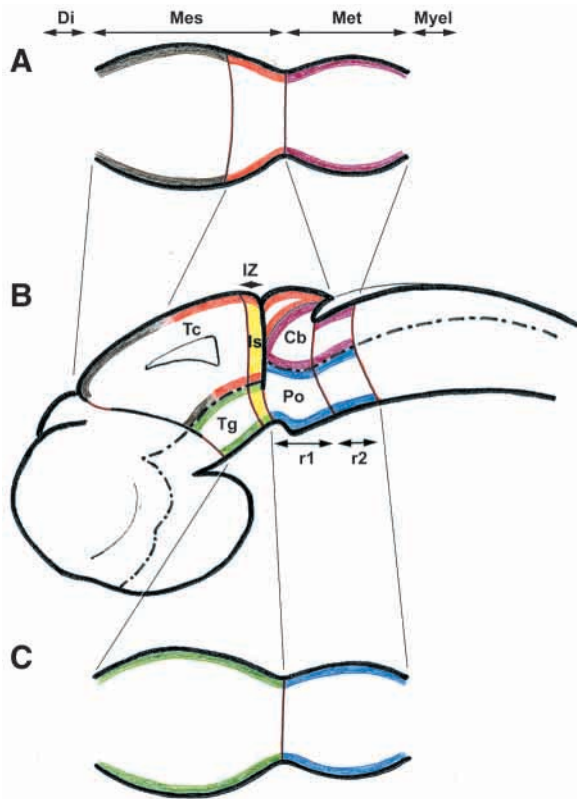


Fig. 1. Schematic organization of the MH domain at the 10-somite stage (A,C) and at 24 hpf (B). All views are anterior towards the left; A and C are dorsal and ventral views of the alar and basal plates, respectively; B is a sagittal view, the broken line delimiting the alar/basal boundary. The early MH domain comprises the mes- and metencephalic vesicles; the contribution of each vesicle to the late MH derivatives, as demonstrated in transplantation experiments in the avian embryo (Hallonet and Le Douarin, 1990; Hallonet et al., 1993; Martinez and Alvarado-Mallart, 1989) (and without considering the floor and roof plates) is color-coded and indicated by the vertical lines: (1) the alar plate of the mesencephalic vesicle contributes to the tectum; (2) in addition, the caudal third of the mesencephalic vesicle is at the origin of the alar part of the isthmus and dorsomedial part of the cerebellar plate (future vermis) and alar part of r2; (3) the alar plate of the metencephalon gives rise to the lateral cerebellum (future hemispheres); (4) the basal plate of the mesencephalic vesicle gives rise to the tegmentum; (5) the basal plate of the metencephalic vesicle gives rise to the pons (basal r1) and basal plate of r2. The isthmus is colored in yellow. Its basal part has not been precisely mapped and was not studied for its inductive properties of MH fate; it is drawn here based on the expression pattern of isthmus organizer markers such as *wnt1* and *fgf8*. The ‘intervening zone’ is defined as the territory delayed in neurogenesis (Geling et al., 2003). It is located at the MHB but its spatial relationship with the isthmus has not been established. Cb, cerebellum; Di, diencephalon; Is, isthmus; IZ, intervening zone; Mes, mesencephalon; Met, metencephalon; Myel, myelencephalon; Po, pons; r, rhombomere; Tc, tectum opticum; Tg, tegmentum.

Bally-Cuif, 2001) (Fig. 1). Among the factors that likely mediate IsO activity are the secreted proteins Fgf8 and Wnt1, expressed on either side of the MHB. Accordingly, genetic analyses in the mouse, chicken and zebrafish demonstrate that a positive crossregulatory loop between the expression of IsO markers, of Pax2/5/8- and of Engrailed-family members is involved, at somitogenesis stages, in the stabilization of identities surrounding the MHB (Martinez, 2001; Rhinn and Brand, 2001; Wurst and Bally-Cuif, 2001).

Transplantation studies further pointed to the remarkable plasticity of MH identities, the regionalisation of which becomes fixed only at a late stage. For example, in the avian embryo, midbrain AP polarity can be regulated until at least 12–13 somites: at that stage, it is corrected following an experimental rotation of the mesencephalic vesicle in ovo (Marin and Puelles, 1994), or is reorganized around ectopic transplants of MHB-containing tissue (Alvarado-Mallart et al., 1990; Gardner and Barald, 1991; Martinez et al., 1991; Nakamura et al., 1988) or around ectopic foci of Fgf8 expression (Crossley et al., 1996; Irving and Mason, 2000; Lee et al., 1997; Martinez et al., 1999). At the same stage, MH identity can also be changed into a diencephalic or more posterior hindbrain specification in misexpression experiments of diencephalic (Pax6) (Matsunaga et al., 2000a) or r2 (Hoxa2) (Irving and Mason, 2000) factors. Further insight into the potentialities of the MH domain will be provided by the analysis of mouse or zebrafish mutants deficient in IsO activity. The zebrafish mutants for Pax2.1 (*no-isthmus*, *noi*) and Fgf8 (*acerebellar*, *ace*) functions are of particular interest, because in these backgrounds molecular MH markers are initially properly induced, but are not maintained (Brand et al., 1996; Lun and Brand, 1998; Reifers et al., 1998). During somitogenesis, strong *noi* alleles progressively loose the tectum, isthmus and cerebellum (Brand et al., 1996; Lun and Brand, 1998). Similarly, *ace* mutants progressively lack the isthmus and cerebellum (Reifers et al., 1998); they only maintain tectal structures, which express low levels of *Eng*, *ephrin-A5a* and *ephrin-A2*, suggesting that they are of anterior identity (Brand et al., 1996; Picker et al., 1999). Currently, several (non-exclusive) interpretations can account for the loss of MH structures in *noi* and *ace* mutants, among which are the death of MH precursors, their conversion to alternative fates (still to be determined) or their decreased proliferation. Understanding the fate of MH precursor cells in these backgrounds would reveal the initial potentialities of the MH anlage and would clarify the role of the IsO on cell fate.

The MH domain is also characterized by a striking profile of neurogenesis, where neuronal differentiation in the immediate vicinity of the MHB (the so-called ‘intervening zone’, IZ) is much delayed compared to other domains of the neural tube (Bally-Cuif et al., 1993; Palmgren, 1921; Vaage, 1969; Wullmann and Knipp, 2000) (Fig. 1). IZ formation is permitted by an active process of neurogenesis inhibition at the MHB (Geling et al., 2003) and, in zebrafish, the bHLH E(spl)-like factor Her5 (M ller et al., 1996) was identified as the crucial element both necessary and sufficient for the formation of the basal IZ domain (Geling et al., 2003). The IZ plays a crucial role in controlling the extent of MH neurogenesis over time.

Understanding the dynamics of MH regional specification and neurogenesis are thus important issues as sustained MH

plasticity correlates with the development of distinct and organized (1) MH derivatives and (2) neurogenesis domains. To approach this question, we chose to focus on the regulation of *her5* expression. Two main reasons motivated our choice. First, *her5* is the earliest known marker of the MH area (Bally-Cuif et al., 2000; Müller et al., 1996), and as such is the best candidate to label most MH precursors from the moment they are induced within the neural plate. If this proves true, tracing the descendants of cells expressing *her5* at its onset thus should provide the best available means of assessing the fate of MH precursors in vivo. Second, because *her5* expression within the IZ crucially controls the neurogenesis process, looking at the regulation of *her5* expression should permit the appreciation of the dynamics of MH neurogenesis progression.

We report here the construction of zebrafish embryos where a stable reporter labels all descendants of *her5*-expressing cells. To maximize our chances of isolating all *her5* regulatory elements, we used in vitro homologous recombination (ET-cloning) (Muyrers et al., 2000; Muyrers et al., 1999; Zhang et al., 1998) to introduce an *egfp* reporter cDNA at the *her5* locus in a PAC containing more than 40 kb of *her5* upstream sequence. We demonstrate in several independent lines that *gfp* expression in transgenic embryos carrying the recombined *her5PAC:egfp* construct faithfully reproduces *her5* transcription at all stages, including the earliest step of *her5* induction. Using the stability of GFP protein as a marker for the descendants of *her5*-expressing cells, we first demonstrate that the earliest *her5*-expression domain at gastrulation encompasses and thus is the first known marker of the whole MH anlage. By comparing the distribution of *her5* RNA and GFP protein, we reveal a dynamic restriction of *her5* expression to the MHB over time, and propose that this phenomenon permits the progression of neurogenesis in a converging manner towards the MHB during MH development. Finally, we use GFP to follow *her5* progeny in the *noi* and *ace* backgrounds. We demonstrate that MH precursor cells are maintained but express alternative identities in *noi* and *ace*, albeit with striking differences between the two mutant contexts. Our results suggest a model for the progressive restriction of potentialities of MH precursors over time, and the respective roles of Pax2.1 and Fgf8 in this process.

MATERIALS AND METHODS

Fish strains

Embryos were obtained from natural spawning of AB wild-type or transgenic fish, *ace^{ti282a}* or *noi^{ti29a}* adults (Brand et al., 1996); they were raised and staged according to Kimmel et al. (Kimmel et al., 1995).

Isolation of *her5*-containing PACs and determination of *her5* genomic structure

Two independent PACs containing the genomic *her5* locus (BUSMP706P0356Q2, BUSMP706H15152Q2) were isolated by PCR from pools of library 706 (RZPD, Berlin) using the following primers: *her5* upstream 5'TAGTAGACCTAGCTGGTCTTTTCAG-TCTTTGGAGAGC3', *her5* reverse 5'TAAAAAGGGCAGCAC-AGAGGAGAGTGATGAGGATGT3', with a 59°C annealing temperature and 30 amplification cycles, producing a specific amplification product of 450 bp. PAC DNA was prepared according

to the Qiagen Large Construct kit protocol. Genomic inserts are flanked by *NotI* sites; digestion with *NotI* followed by pulse field gel electrophoresis (PFGE) revealed that the inserts of both PACs were above 100 kb. Further restriction analyses and Southern blotting revealed that PAC BUSMP706H15152Q2 contained more than 40 kb of upstream *her5* sequence; this PAC was chosen for further experiments. The genomic structure of *her5* (Fig. 2A) was determined by PAC sequencing, and was verified on the endogenous *her5* locus by PCR amplification and sequencing of genomic DNA.

ET cloning

ET cloning was based on the protocol provided by Stewart, available on the ET cloning web page <http://www.heidelberg.de/ExternalInfo/stewart/ETprotocols.html>.

Vectors used

pEGFP-1 (Clontech); *pSV40/Zeo* (Invitrogen); *pGLI3_3* (modified *pEGFP-1* with a *loxP*-flanked *Zeo*-cassette in *AflIII*-site, see below); *pGETrec*, carrying arabinose-inducible *recE* gene (Narayanan et al., 1999); *p705-Cre* (Buchholz et al., 1996); and *her5*-containing PAC (*pCYPAC2n* backbone) with a total of about 100 kb genomic insert and at least 40 kb upstream region of *her5*, further called *her5PAC*.

Construction of *pGLI3_3*

pEGFP-1 was digested with *AflIII*, and an insert containing *loxP* and the restriction enzyme site *NheI* (produced by oligonucleotide annealing) was inserted at this site. Similarly, a *loxP-NheI* was introduced into the vector *pSV40/Zeo* after restriction cutting with *BamHI*. *pSV40/Zeo:loxP-NheI* was further cut with *NheI* to release the *NheI* fragment containing full length of *Zeo^R* and *loxP*, which was inserted into *pEGF:loxP-NheI* open at *NheI*. This produced *pEGFP:loxP-Zeo^R-loxP*, further referred to as *pGLI3_3*. All plasmids containing *Zeo^R* were grown in INF α F' cells.

Preparation of the linear fragment *her5a-EGFP:loxP-Zeo^R-loxP-her5b* to homologously recombine into the PAC

Primer design

The fragment for homologous recombination was prepared by PCR using the following primers. Primer ET2: 48 nucleotides specific to the 5'-sequence of *her5* exon 2 (Fig. 2A, fragment b) and 21 nucleotides specific to *pGLI3_3* (underlined) (sequence: 5'GTC CCC AAG CCT CTC ATG GAG AAA AGG AGG AGA GAT CGC ATT AAT CAA GTC GCC ACC ATG GTG AGC AAG3'). Primer ET1: 47 nucleotides specific to the 3'-sequence of *her5* exon 2 (Fig. 2A, fragment b) and 22 nucleotides specific to *pGLI3_3* (underlined) (sequence: 5'CTC ATT GTT TGT GTT CTC AAG TAA AAG CAT TCT CAA GGT TTC TAG GCT TAA CGC TTA CAA TTT ACG CCT3').

Oligonucleotide purification

Oligonucleotides ET1 and ET2 were resuspended in water and purified as follows. To 100 μ l, 12 μ l 3 M Sodium-Acetate (pH 7.5) and 120 μ l phenol were added, vortexed and centrifuged for 3 minutes. Then 360 μ l Ethanol was added, and the mix was placed 10 seconds at 80°C, washed once with 75% ethanol, dried and finally dissolved in 100 μ l water.

PCR amplification of the fragment *her5a-EGFP:loxP-Zeo^R-loxP-her5b*: Template *her5PAC* DNA was denatured for 2 minutes at 94°C, followed by two cycles of denaturation at 94°C for 40 seconds. A first, annealing was performed at 62°C for 30 seconds, with extension at 72°C for 2 minutes. This was followed by 35 amplification cycles with denaturation at 94°C for 40 seconds, annealing at 58°C for 30 seconds, extension at 72°C for 2 minutes. The reaction was stopped by a final extension at 72°C for 10 minutes and cooled at 4°C. The expected 2 kb amplification product was purified using the QIA gel extraction kit (Qiagen) as recommended, and eluted in 50 μ l water.

Preparation of bacterial cells and transformation

The bacterial host cells DH10B containing *her5PAC* were transformed with *pGETrec* and prepared for the recombination with the linear *her5a-EGFP:loxP-Zeo^R-loxP-her5b* fragment as follows: starting from an overnight culture, the cells were grown at 37°C for 90 minutes (to OD₆₀₀=0.2–0.3) with shaking. L-arabinose was added to the culture to a final concentration of 0.2% and the culture was grown further until OD₆₀₀=0.5 was reached. The cells were then prepared as electro-competent as described in <http://www.heidelberg.de/ExternalInfo/stewart/ETprotocols.html>. Electroporation of 120 ng of *her5a-EGFP:loxP-Zeo^R-loxP-her5b* fragment was performed with 2.5 kV pulses and 25 µF in 100 µl, induced with 0.2% L-arabinose at 37°C for 90 minutes before harvesting and plating twice for selection.

Removal of *loxP*-flanked *Zeo^R*-gene by Cre-mediated deletion

Competent cells carrying the recombined *her5PAC* were transformed with *p705-Cre* using standard protocols. *p705* is based on the *pSC101* temperature-sensitive origin, which maintains a low copy number and replicates at 30°C but not at 40°C. Furthermore, *Cre* is expressed from the *lambdaPR* promoter weakly at 30°C and strongly at 37°C. Finally, these plasmids are lost from cells if incubated at temperatures above 37°C. Thus, after transformation the cells were incubated for 2 days at 30°C, followed by 1 day's incubation at 40°C to give a transient burst of *Cre* expression after which the plasmids will be eliminated from the cell. The cells were then further grown for day at 37°C, transferred once and finally tested by PCR for excision of the *loxP-Zeo^R-loxP* cassette, generating *her5PAC:egfp*. Because of the presence of a *NotI* site 3' to the *egfp* gene, digestion of *her5PAC:egfp* with *NotI* generated two fragments of 45 and 60 kb in addition to the vector backbone. PFGE and Southern blotting with a *her5* probe identified the 45 kb fragment as containing the coding *her5* sequence, thus *her5PAC:egfp* contains more than 40 kb upstream *her5* sequence driving *egfp* expression.

Construction of *her5PAC:egfp* deletion fragments

The fragment containing 3650bp of *her5* upstream sequence was obtained by digestion of *her5PAC:egfp* with *NotI* + *BglII* followed by pulse field gel electrophoresis, identification by Southern blotting with a probe covering the *her5* 5' region, and gel purification (Qiagen Gel extraction kit). The fragment was subcloned into *pBS(SK)* for amplification, and was repurified by digestion and gel extraction before injection. All other constructs were prepared as PCR fragments from *her5PAC:egfp* and purified using the Qiagen PCR purification kit. All fragments were eluted in H₂O (Ambion).

Construction of the transgenic lines

her5PAC:eGFP DNA was isolated using the Qiagen Large Construct Kit, eluted in H₂O and injected (in circular form) into fertilized eggs at the one-cell stage at a concentration of 50 ng/µl. All other constructs were injected as linear fragments at the same concentration. Injected embryos were raised to adulthood and mated to wild-type adults. F1 embryos expressing eGFP were then sorted-out, raised and crossed to wild-type fish to establish the lines. We obtained integration and expression in three from 600 injected fish for *her5PAC:egfp* and in average three from 50 injected fish for the other fragments. All results presented in this work were verified over at least three generations.

In situ hybridisation and immunocytochemistry

In situ hybridisation and immunocytochemistry were carried out according to standard protocols (Hauptmann and Gerster, 1994). The following in situ antisense RNA probes were used: *her5* (M ller, 1996; Thisse et al., 1993); *egfp* (Clontech); *pax6* (Krauss et al., 1991); *fgfr3* (Sleptsova-Friedrich et al., 2002); *otx2* (Li et al., 1994b); *hoxa2* (Prince et al., 1998); and *krx20* (Oxtoby and Jowett, 1993).

For immunocytochemistry, the following antibodies were used:

mouse anti-GFP 'JL-8' (Chemicon) used at a dilution of 1/100; mouse anti-injected 4D9 (DHSB), which recognises all zebrafish Eng proteins, used at a dilution of 1/8; and rabbit anti-phosphohistone H3 (Upstate Biotechnology, no.06-570) used at a dilution of 1/200. They were revealed using goat-anti-mouse-HRP or goat-anti-rabbit-HRP (Chemicon) (dilution 1/200) followed by DAB/H₂O₂ staining, or goat-anti-mouse-FITC (Dianova) (dilution 1/200), as appropriate. Double in situ hybridisation and immunocytochemistry staining on transgenic embryos were performed as follows: whole-mount embryos were first processed for in situ hybridisation, then cryostat-sectioned at 8 µm thickness and the sections were subjected to immunocytochemistry following standard protocols. In Fig. 7K–M, immunocytochemical detection was performed after in situ hybridisation on whole-mount specimen. Embryos were scored and photographed under a Zeiss SV11 stereomicroscope or a Zeiss Axioplan photomicroscope.

Fate mapping of the anterior and posterior extremities of the early *her5*-positive domain

her5PAC:egfp transgenic embryos were injected at the one-cell stage with 7 mg/ml DMNB-caged fluorescein (10 kDa, Molecular Probes), and were left to develop in the dark. When GFP protein first became visible (at 95% epiboly), small groups of four or five cells located within the most anterior or most posterior rows of GFP-positive cells (see yellow and red dots on Fig. 5A) were UV-irradiated for 2 minutes using DAPI illumination and a 0.1 mm pinhole under a 63× water objective, according to Kozłowski and Weinberg (Kozłowski and Weinberg, 2000). Embryos were fixed at 24 hpf and uncaged fluorescein was detected by immunocytochemistry as described by Dickmeis et al. (Dickmeis et al., 2001).

Acridine Orange staining

For characterization of cell death, embryos were stained according to Williams and Holder (Williams and Holder, 2000), with minor modifications. Briefly, embryos were incubated for 20 minutes in 5 µg/ml Acridine Orange (Sigma) in embryo medium, washed three times for 5 minutes in embryo medium and observed under fluorescence microscopy with FITC filter.

RESULTS

gfp transcription in *her5PAC:egfp* transgenic lines faithfully reproduces all phases of embryonic *her5* expression

Because gene regulatory elements might be located at a distance from the transcriptional start site, we chose to search for *her5* enhancers using a homologous recombination approach in large genomic fragments. Two PACs were isolated that contained the genomic *her5* locus, and the PAC insert containing the longest 5' sequence (over 40 kb, as determined from pulse field gel electrophoresis and Southern blotting) was selected. We found that the complete *her5* coding sequence overlaps three exons, where exon 1 contains the transcription start site and encodes the 17 N-terminal Her5 amino acids (Geling et al., 2003). Exon 2 codes for the 32 following amino acids, comprising the basic domain, helix 1 and part of the loop domain of Her5 (Fig. 2A), and exon 3 for the last 165 amino acids. We used the ET-cloning technology (Muyers et al., 2000; Muyers et al., 1999) to recombine the *egfp* cDNA in frame after amino acid 33 of Her5 (end of the basic domain) (Fig. 2A). The *egfp* cDNA was terminated with a stop codon and polyadenylation signal, thus translation of the recombined mRNA is stopped after a fusion protein that does not comprise the protein interaction motifs of Her5 (HLH

and more C-terminal domains). We expected that this fusion protein would not interfere with the activity of other bHLH factors. In line with this prediction, we did not detect any morphological or molecular phenotype in all our transient or stable expression assays (see below, and data not shown). Three independent transgenic lines were established that carried the recombinant *her5* PAC (*her5PAC:egfp* lines). All showed an identical *gfp* RNA expression profile at all embryonic stages examined (data not shown). These lines will be used indiscriminately below.

At early gastrulation, *her5* is transcribed in a subset of anterior endodermal precursors ('e' in Fig. 2C) (Bally-Cuif et al., 2000). Accordingly, we detected GFP expression in the pharynx at 24 hours post-fertilization (hpf) (Fig. 2D, Fig. 3) in all *her5PAC:egfp* embryos. These results make of *her5* the earliest selective pharyngeal marker known to date, and are in line with the proposed role of endodermal Her5 activity in attributing pharyngeal fate (Bally-Cuif et al., 2000). In addition, wild-type *her5* expression is initiated at the 70% epiboly stage in a V-shaped neuroectodermal domain ('MH' in Fig. 2C) that was fate-mapped to the midbrain at 90% epiboly (Müller et al., 1996). Accordingly, strong GFP expression was found in the MH domain (Figs 2D and 3).

The early control of MH *her5* expression involves two distinct phases: expression is initiated at 70% epiboly by currently unknown regulators, and is maintained and refined after the five-somite stage by the MH regulatory loop (Lun and Brand, 1998; Reifers et al., 1998). To determine whether *egfp* transcription was a faithful reporter of *her5* expression, we performed double in situ hybridisation experiments with *gfp* and *her5* probes on *her5PAC:egfp* embryos between 60% epiboly and 24 hpf. *her5PAC*-driven *gfp* transcription faithfully reproduced expression of endogenous *her5* at all embryonic stages tested, both in its onset and spatial extent (Fig. 3A,C,D, and data not shown). In particular, *gfp* expression was initiated at 70% epiboly within the neural plate and maintained in the MH domain thereafter, demonstrating that both the initiation and maintenance phases of *her5* transcription are recapitulated by expression of the transgene. Together, these observations demonstrate that the *her5PAC* construct comprises all the regulatory elements that control endogenous *her5* expression at embryonic stages.

Distinct positive and negative regulatory elements controlling endodermal and neural expression of *her5* are organized over 3 kb of upstream sequence

To narrow down the sequences directing MH and/or endodermal expression of *her5*, we performed a deletion analysis series of the *her5PAC:egfp* transgene. A comprehensive series of reporter constructs of varying length encoding the Her5-eGFP fusion protein and comprising between 60 and 3650 bp upstream of the *her5* transcriptional start site (Geling et al., 2003) were amplified by PCR from *her5PAC:egfp* and tested in transient or transgenic assays (black or red lines in Fig. 2B, respectively). In the latter case, at least two independent lines were established for each construct. Transient assays generally produced ectopic expression sites when compared with transgenic analyses of the same fragments; however, comparison of a sufficient number of injected embryos ($n > 30$) allowed to reliably predict

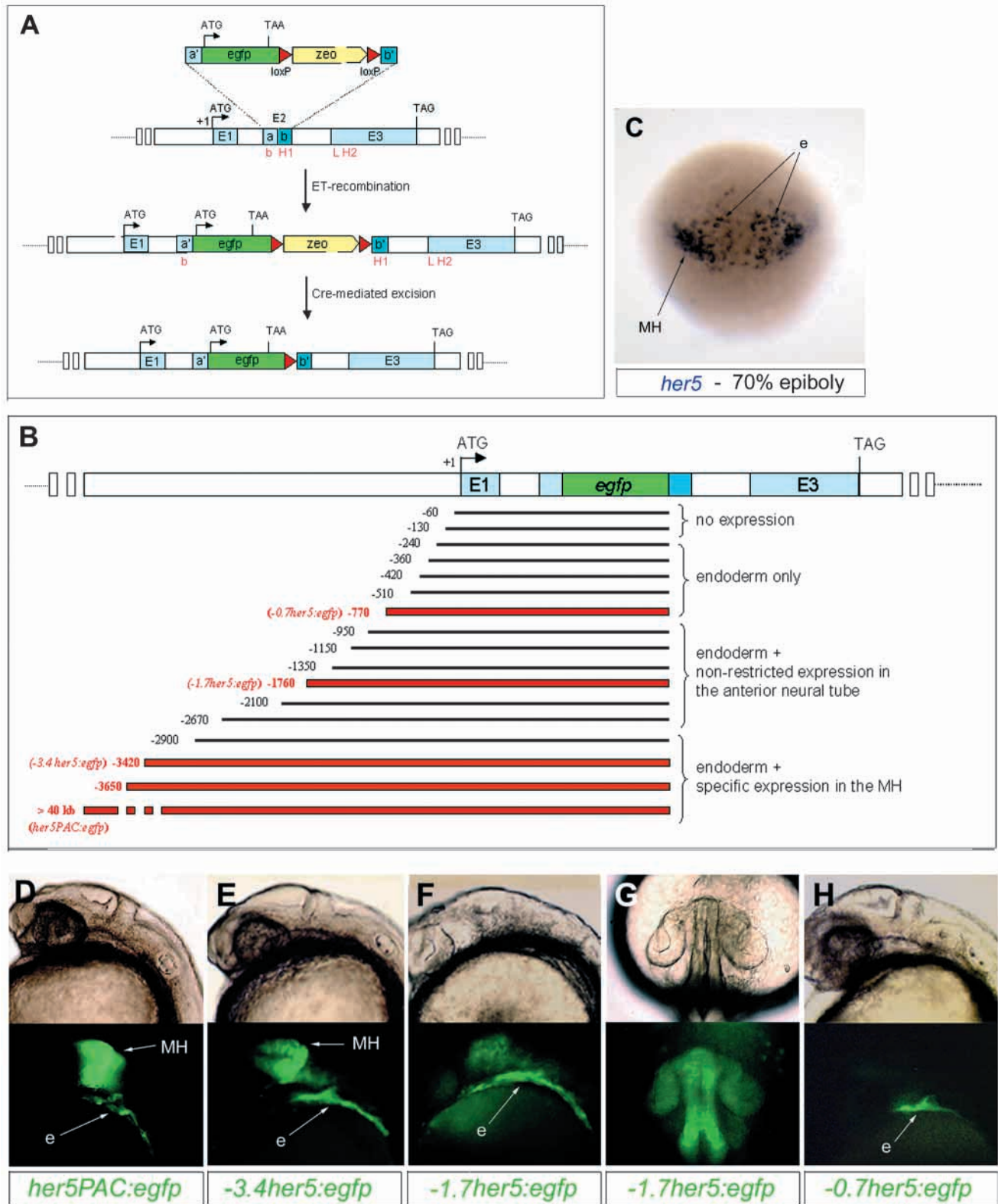
the reporter expression profile (not shown). All results are summarized in Fig. 2B,D. In summary, we observed that all fragments containing 240 bp or more of upstream sequence lead to non-neural expression (Fig. 2B). Transgenic lines established with 770 bp upstream region ($-0.7her5:egfp$) faithfully recapitulated *her5* endodermal expression, with similar onset and anteroposterior extent (Fig. 2D-H and data not shown). These results locate the *her5* endodermal enhancer to the first upstream 770 bp, the first *her5* intron (contained in all constructs) or a combination of both.

We next examined the regulatory elements controlling neural expression of *her5*. We found that all constructs containing more than 770 bp of upstream sequence directed, in addition to endodermal expression, GFP fluorescence within the neural tube (Fig. 2D-G). However, MH selectivity in stable assays was only achieved with upstream sequences of 3.4 kb or more ($-3.4her5:egfp$ lines) (Fig. 2E), whereas shorter elements triggered GFP expression over the MH as well as fore- and hindbrain (e.g. $-1.7her5:egfp$ lines, Fig. 2F,G). Double in situ hybridisation experiments with *gfp* and *her5* probes demonstrated that *gfp* transcription in $-3.4her5:egfp$ transgenics faithfully reproduces expression of endogenous *her5*, including its induction and maintenance phases (Fig. 3B,E,F, and data not shown). Thus, all regulatory elements driving correct MH *her5* both in time and space appear contained within the $-3.4her5:egfp$ construct. Together, our analysis of the *her5* enhancer demonstrates that spatially distinct and dissociable elements drive endodermal and MH expression of *her5* during embryogenesis.

her5 expression in endodermal precursors is initiated at 30% epiboly, and switched off at 90% epiboly (Bally-Cuif et al., 2000). We could detect GFP protein in the pharynx until 26-30 hpf (e.g. see Fig. 2D,F,H), thus GFP protein is stable for ~18-20 hours in this tissue in our lines. We reached a similar conclusion for GFP stability in the neural tube, where posterior *her5*-positive cells at 75% epiboly rapidly switch off *her5* expression and give rise to metencephalic derivatives that lose GFP protein around 24 hpf (see below). Thus, the GFP protein profile observed at a given time corresponds to all descendants of the cells that expressed *gfp* under *her5* regulatory elements between 18-20 and a few hours before the moment of analysis. The stability of the GFP protein in *her5PAC:egfp* embryos thus offers the unique opportunity of following the fate of *her5*-expressing cells, from the onset of endogenous *her5* expression and throughout embryogenesis.

Neural *her5* expression at gastrulation encompasses the entire MH anlage

The MH anlage is composed of precursors for the midbrain, isthmus, r1 and r2 (Fig. 1). These domains are together characterized by the expression of Eng2 proteins at somitogenesis stages, but an early molecular marker of the entire presumptive MH remains to be identified. The onset of *her5* expression within the neural plate is at 70% epiboly, and GFP protein becomes visible in this location around 90% epiboly (not shown). To determine the fate of these early *her5*-expressing cells, we performed a detailed spatiotemporal analysis of GFP distribution by fluorescence microscopy on live embryos and immunocytochemistry on whole-mount or sectioned specimen (Fig. 4A-J). When necessary, GFP protein



distribution was compared with the expression of diagnostic molecular markers for diencephalic (see Fig. 8A,E,G,I) or hindbrain domains (Fig. 4K-Q).

The morphological constriction marking the midbrain-hindbrain boundary (MHB) becomes visible from the 10-12-

somite stage onwards, and is prominent by 20 somites (Fig. 4E, arrow). At the 12- and 20-somite stages, GFP protein clearly distributes over the entire midbrain as well as posterior to the MHB (Fig. 4A,C,E), and a cross-section at the MHB level demonstrates that all neural tube cells are stained (Fig. 4B,

Fig. 2. Structure of the *her5* genomic locus and reporter constructs and corresponding GFP expression. (A) Construction of *her5PAC:egfp* by ET-cloning-mediated recombination of the *egfp* cDNA within exon 2 of *her5*. The *her5* locus comprises 3 exons (blue), of which exon 2 encodes the basic and first helix domain of the Her5 protein (bHLH domain labeled in red as b, H1, L and H2). Recombination arms (a', b') matching exon 2 were amplified in frame with the *egfp* sequence and a floxed zeocine resistance cassette (*zeo*) (top construct). The resulting product was inserted in vitro within a *her5*-containing PAC by ET-mediated homologous recombination (Muyrers et al., 2000; Muyrers et al., 1999). The *zeo* cassette was subsequently deleted by Cre excision in vitro, generating the *herPAC:egfp* construct (bottom line). (B) Reporter constructs used to localise *her5* regulatory elements in transient (black lines) or transgenic (red lines) assays. Most constructs were generated from *her5PAC:egfp* (bottom construct) by PCR amplification and contain *egfp* in frame within *her5* exon 2. Numbering to the left of each fragment refers to the length of upstream sequence from the transcriptional start site, in bp. The expression profile driven by each construct is written to the right. Note that the enhancer element(s) driving endodermal expression are located within 240 bp of upstream sequence and/or intron 1, and that sequences driving specific MH expression are recovered with 2.9 kb of upstream sequence. (C) Endogenous *her5* transcription at 70% epiboly (onset of neural *her5* expression) revealed by whole-mount in situ hybridisation (blue staining). *her5* is expressed in a V-shaped domain at the AP level of the MH anlage (MH) and in a subset of anterior endodermal precursors (e) (see also Bally-Cuif et al., 2000). (D-H) Selected examples of GFP protein expression driven by representative reporter constructs [bright field (top) and fluorescent (bottom) views of transgenic embryos, constructs as indicated below each panel]. All constructs illustrated drive expression to the anterior endoderm. Constructs comprising more than 2.9 kb of upstream sequence (D,E) drive selective neural expression to the MH. Intermediate constructs (F,G) drive unrestricted anterior neural expression.

top). Whole-mount analyses and lateral sections further reveal intense GFP staining in neural crests streams that exit the midbrain area towards anterior and ventral (Fig. 4C,D). At 25 somites and later, the isthmus fold has formed and the cerebellar anlage is discernible. GFP protein is detected in the midbrain, isthmus, cerebellar fold and pons (Fig. 4F-H, see also Fig. 6A,B). The intensity of GFP staining in the metencephalon is, however, weak compared with midbrain expression, and becomes undetectable after 26 hpf (Fig. 4I). GFP expression at 26 hpf remains prominent in the midbrain, albeit with a clear caudorostral decreasing gradient. After 30 hpf, GFP protein is maintained only at the MHB (Fig. 4J), in a profile reminiscent of late *her5* RNA transcription (see Fig. 6C).

To position precisely the spatial limits of GFP protein distribution, we compared its anterior and posterior borders with the expression of diagnostic markers. *pax6.1*, the zebrafish ortholog of murine and chicken *Pax6*, is expressed within the anterior alar plate with a posterior limit at the di-mesencephalic boundary (Li et al., 1994a; Macdonald et al., 1995). From the onset of *pax6.1* expression (12 somites) until at least the 30-somite stage, we found that GFP- and *pax6.1*-positive cells precisely abut each other at the di-mesencephalic border (Fig. 8A,C,E,G). The posterior extent of GFP protein distribution was determined by comparison with the expression of *hoxa2* from 10 somites onwards, when *hoxa2* exhibits a sharp anterior limit of expression at the r1/r2 boundary (Prince

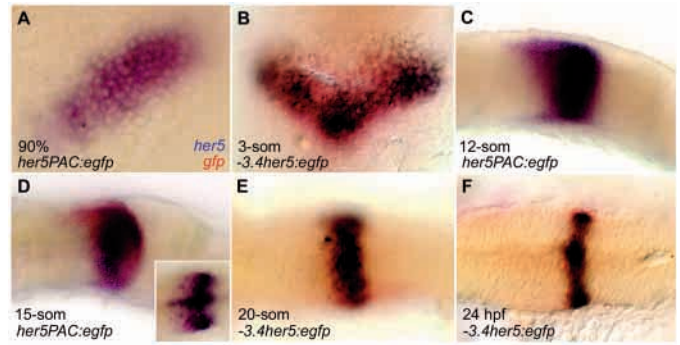


Fig. 3. Comparison of endogenous *her5* (blue) and *gfp* (red) RNA transcription profiles in *her5PAC:egfp* (A,C,D) and *-3.4her5:egfp* (B,E,F) transgenic embryos, at the stages indicated. All views are high magnifications of the MH area in flat-mounted embryos, dorsal (A,B,E,F and inset in D) or sagittal (C,D) orientations, anterior towards the top (A,B) or left (C-F). Endogenous *her5* and *gfp* expressions exactly coincide at all embryonic stages, including the initiation (A,B) and maintenance (C-F) phases of *her5* transcription, demonstrating that all the regulatory elements driving MH *her5* expression are contained within the *her5PAC:egfp* and *-3.4her5:egfp* constructs.

et al., 1998), and with the expression of *krox20* that marks r3 and r5 (Oxtoby and Jowett, 1993). At 10 somites and subsequent stages until at least 30 somites, GFP distribution overlaps r2 (Fig. 4K,M,O,Q). A few GFP-positive cells can also transiently be found within r3 and r4 at 10 somites (Fig. 4L). At this stage, cells in r3 co-express GFP protein and *krox20* (Fig. 4N, yellow arrows). However the contribution to r3 and r4 is marginal and no longer detectable at 20 somites (Fig. 4P).

To ascertain that *her5* expression at its onset within the neural plate comprises all MH precursors, we determined whether the spatial organization of the earliest *her5*-expressing cells prefigures the later distribution of MH cells along the AP axis. To this aim, we fate mapped the anterior and posterior extremities of the *her5* domain at 70% epiboly. To reliably identify this domain, we relied on its giving rise to the earliest detectable GFP expression using fluorescence microscopy in *her5PAC:egfp* embryos, at 90-95% epiboly. Thus we activated caged-fluorescein in small groups of four or five GFP-positive cells located at the edges of the GFP domain in transgenic embryos at 95% epiboly (Fig. 5A), and followed these cells at 24 hpf (Fig. 5B-E). We found that anterior activated cells always gave rise to cell clones distributing within the anterior midbrain (Fig. 5B,C) ($n=4$), while posterior activated cells populate r2 (Fig. 5D,E) ($n=5$). Thus, the anterior and posterior extremities of the earliest *her5*-expressing domain at 70% epiboly prefigure the corresponding extremities of the later MH.

Together, our findings demonstrate that the early neural expression of *her5* is a marker of the entire MH anlage, and it appears as the earliest MH marker known to date. Furthermore, this early domain displays some degree of ordered cell distribution, such that its anterior and posterior limits contain precursors for the anterior and posterior extremities of the later MH. Specifically, at 70% epiboly, anterior *her5*-positive cells abut and exclude the diencephalon anlage, while posterior cells comprise precursors for r1 and r2.

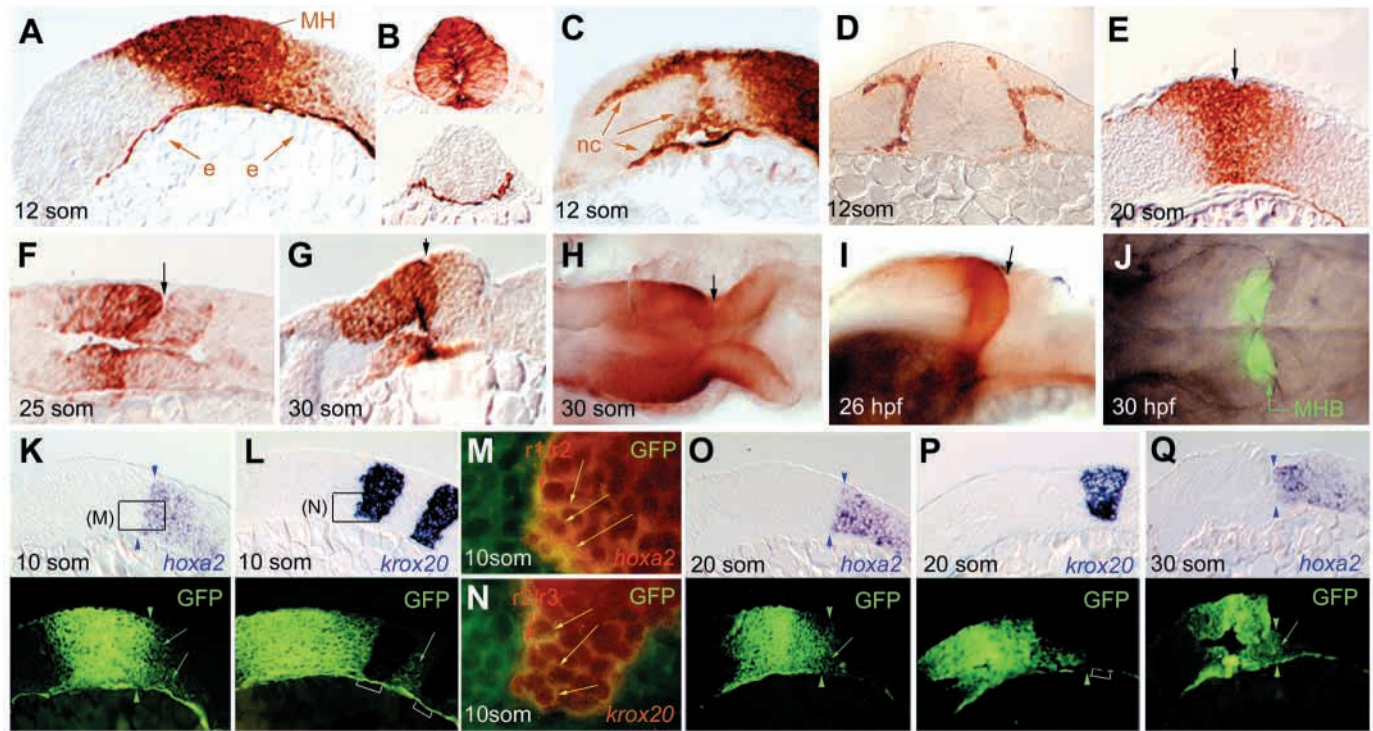


Fig. 4. The distribution of GFP protein in *her5PAC:egfp* embryos reveals the fate of endodermal and neuroectodermal cells expressing *her5* at gastrulation. GFP protein in *her5PAC:egfp* embryos was observed on live specimen (J) or revealed by immunocytochemistry (A-I, brown DAB staining; and K-Q, green FITC staining) at the stages indicated (bottom left of each panel). (H-J) Whole-mount views: (H,J) dorsal views, anterior leftwards; (I) lateral view, anterior leftwards. (K-Q) Sagittal sections, anterior leftwards. In K,L,O-Q, the top and bottom panels are bright-field and fluorescent views, respectively, of the same sections that were each processed for in situ hybridisation (top panels, blue staining, probes indicated in the bottom right-hand corner) and immunocytochemistry against GFP protein (bottom panels). (M,N) High magnifications of levels equivalent to those boxed in K and L, respectively (red arrows indicate rhombomere boundaries). Overlay pictures of the in situ hybridisation staining (revealed using Fast Red, red fluorescence) and GFP immunocytochemistry (FITC staining). The cytoplasm of cells doubly positive for GFP protein and for the in situ hybridisation marker (*hoxa2* or *krox20*, respectively) appears yellow. The descendants of endodermal *her5*-expressing cells distribute to the entire AP and mediolateral extent of the pharynx (A; cross-section at hindbrain level in B, bottom). At 12 somites, the descendants of neural *her5*-expressing cells distribute over a broad domain at the level of the MH (A; cross-section at forebrain level in B, top). Neural crest cells that exit the MH are also GFP-positive (C, note a dorsal stream and a stream caudal to the eyes, and cross-section at forebrain level in D). In E-J, arrows indicate the midbrain-hindbrain boundary; note that GFP protein distributes posterior to this level (i.e. to metencephalic derivatives) until 24 hpf, and encompasses r2 (K,O,Q; blue and green arrowheads to the anterior limit of *hoxa2* expression; green arrows to GFP-positive cells in r2), with a minor contribution to r3 and r4 before the 20-somite stage (L,P; white brackets indicate r3 and r5, green arrow in L indicates GFP cells in r4; green arrowhead in P indicates the posterior limit of GFP extension at the r2/r3 boundary). At 10 somites, GFP-positive cells in r2 and r3 co-express *hoxa2* and *krox20*, respectively (yellow arrows in M,N). e, endoderm; hg, hatching gland; MH, midbrain-hindbrain domain; MHB, midbrain-hindbrain boundary; nc, neural crests streams.

***her5* expression follows a dynamic mode of regulation that is precisely controlled in time and space**

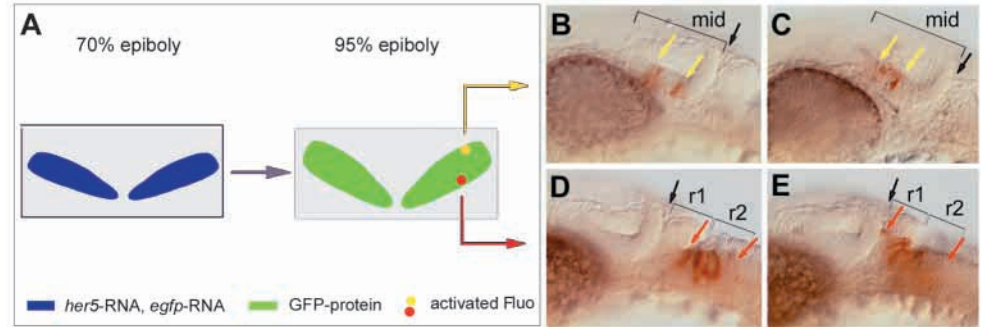
Her5 crucially controls MH neurogenesis (Geling et al., 2003), making it important to analyze the regulation of its expression. In 30-somite *her5PAC:egfp* embryos, we observed a dramatic difference in the AP extent of *her5* transcription and GFP protein distribution (Fig. 6A-C). This observation suggests that MH precursors loose *her5* expression upon division, such that the *her5*-positive territory shrinks from a domain covering the entire MH anlage at early gastrulation, to be maintained at 30 somites at the MHB only. To confirm this hypothesis, and assess the progression of this phenomenon in time and space, we conducted a precise comparison of *her5* RNA and GFP protein distributions between 90% epiboly (first stage where GFP protein becomes detectable in the MH domain) and

24 hpf. To this aim, double in situ hybridisation and immunocytochemical detection was performed on whole-mount embryos or serial sagittal sections (minimum three embryos per stage). At 90% epiboly and until the one- to two-somite stage, the anterior borders of *her5* RNA and GFP protein expression were coincident (Fig. 6D, and data not shown). However their posterior limits differed by approximately one or two cell rows (Fig. 6D, and data not shown). Thus, between the onset of *her5* expression in the neural plate (70% epiboly) and 90% epiboly, *her5* transcription becomes restricted of a few cell rows posteriorly, although it is maintained in all its progeny cells anteriorly (Fig. 6P, parts a,b). At three somites, *her5* transcripts distribute over approximately eight cell rows along the AP axis, while GFP protein covers 15-18 rows (Fig. 6E,F). From this stage onwards, prominent differences in the AP extent of *her5* RNA

Fig. 5. The earliest *her5*-positive domain at gastrulation contains an ordered distribution of MH precursors and prefigures the later MH domain.

(A) Experimental approach. The earliest *her5*-positive domain (schematized in blue on a dorsal view of the neural plate at 70% epiboly, left panel) is reflected by GFP protein expression starting at 95% epiboly (green, right panel). Thus, the anterior and posterior extremities of the early *her5*-positive domain were fate

mapped by laser activation of caged fluorescein within the most anterior or posterior GFP-positive cell rows at 95% epiboly (yellow and red dots, respectively). (B-E) Location of cells activated in A, revealed at 24 hpf by whole-mount anti-fluorescein immunocytochemistry (brown staining) (all embryos anterior leftwards, with black arrow to the midbrain-hindbrain boundary). (B,C) Anterior activations give rise to cell clones distributing within the anterior midbrain (two different embryos are shown, brackets to the midbrain, yellow arrows to delimit the cluster of uncaged cells). (D,E) Posterior activations produce cell clones located posterior to the midbrain-hindbrain boundary and populate r2 (two different embryos are shown, brackets to r1 and r2, red arrows to delimit the cluster of uncaged cells). mid, midbrain; r1-2, rhombomeres 1-2.



and GFP protein are detectable posteriorly but also anteriorly, on the lateral and basal domains of the midbrain (Fig. 6E, black arrows). By contrast, *her5* expression still mostly matches GFP staining along the dorsal midline of the neural tube (Fig. 6E, blue arrow). Similar observations can be made until the 12- to 14-somite stage (Fig. 6G,H). At 16 somites, the dorsal expression of *her5* dramatically regresses and *her5* expression is restricted to a band of 4-6 cell rows across the entire DV extent of the neural tube (Fig. 6I). At this stage, MH cells have further divided as GFP protein extent now covers approximately 27-30 rows along AP (Fig. 6J). This progression is ongoing at least until the 30-somite stage, when GFP protein extends over 45-50 rows, against 3-5 rows for *her5* RNA (Fig. 4H, Fig. 6K,L).

To ascertain the directionality of the progressive restriction of *her5* expression in MH precursors, we revealed *her5* RNA and GFP protein on single sagittal sections in double fluorescence experiments (Fig. 6M-O). Such stainings unambiguously located the final *her5* expression domain to the center of the GFP-positive domain, confirming that *her5* expression is lost both anteriorly and posteriorly upon cell divisions. Several other MH markers, e.g. *pax2.1*, *eng1*, *wnt1* and *fgf8*, display an expression profile that globally compares in extent with *her5* at early and late stages, and GFP distribution in *pax2.1:gfp* transgenics (Picker et al., 2002) and *wnt1:gfp*-injected embryos (Lekven et al., 2003) suggests that the expression of these genes follow a restriction similar to *her5* over time.

We conclude from these observations that (1) *her5* expression within the MH domain is subject to a highly dynamic regulation and is progressively lost upon cell divisions between 70% epiboly and 24 hpf (Fig. 6P), (2) the restriction of *her5* expression occurs in a centripetal manner towards the MHB, and (3) it follows a precise spatial sequence: it is initiated posteriorly (in the future metencephalon) before affecting the basolateral and finally the dorsal mesencephalic areas. *her5* expression, at least in the basal plate, is always adjacent to neurogenesis sites (Geling et al., 2003). Thus, our observations imply that neurogenesis within the MH domain is also a spatially dynamic process, and converges towards the MHB over time (red arrows in Fig. 6P, part d).

Most MH precursors are maintained but acquire distinct alternative identities in *noi* and *ace* mutant backgrounds

We next used the stability of the GFP protein to study the potentialities of MH precursors in terms of their spatial identity. MH precursors remain plastic until late stages, and the choice and reinforcement of their specification are incompletely understood. We addressed the role of *Pax2.1* and *Fgf8* in these processes, by studying GFP distribution in *noi* and *ace* mutants, where the fate of the presumptive MH anlage is unknown.

We first ascertained that GFP protein could be used as a reliable marker of MH fate in *noi* and *ace*. To this aim, we verified that *gfp* transcription faithfully recapitulated *her5* expression in these mutant contexts. Double in situ hybridisations with the *her5* and *gfp* probes were performed on transgenic mutant embryos, and demonstrated an identical initiation (not shown) and later downregulation of *her5* and *gfp* transcription in these backgrounds (Fig. 7A-D). Near-complete downregulation of *gfp* expression was observable at 24 hpf in *her5PAC:egfp;ace* embryos (Fig. 7B) and at the 10-somite stage in *her5PAC:egfp;noi* (Fig. 7D), like expression of endogenous *her5*. We conclude that the distribution of GFP protein can be used as a faithful tracer of MH precursors in the *ace* and *noi* contexts.

Live observation of 24 hour-old transgenic mutant embryos first revealed that a significant number of GFP-positive fluorescent cells was maintained at that stage in both the *ace* and *noi* backgrounds (Fig. 7E-G). These cells distribute over an AP territory that approaches wild-type size (compare Fig. 7F,G with 7E), and throughout the entire DV extent of the neural tube. No signs of aberrant cell migration were apparent at any stage, i.e. no patches of unstained cells were observed within the GFP-positive domain, and conversely, no patches of positive cells were found outside the main GFP-positive domain. In addition, at 15 somites, no difference was observed in the rate of cell death (as revealed with Acridine Orange) (25 ± 12 cells in wild-type, 26 ± 9 cells in *ace*, 30 ± 5 cells in *noi*; $n=20$) (Fig. 7H-J) and cell proliferation (anti-phosphohistone H3) (61 ± 9 cells in wild-type, 55 ± 6 cells in *ace*; 59 ± 8 cells in *noi*; $n=10$) (Fig. 7K-M) in that area between wild-type, *ace* and *noi* embryos. Together, these observations suggest that the

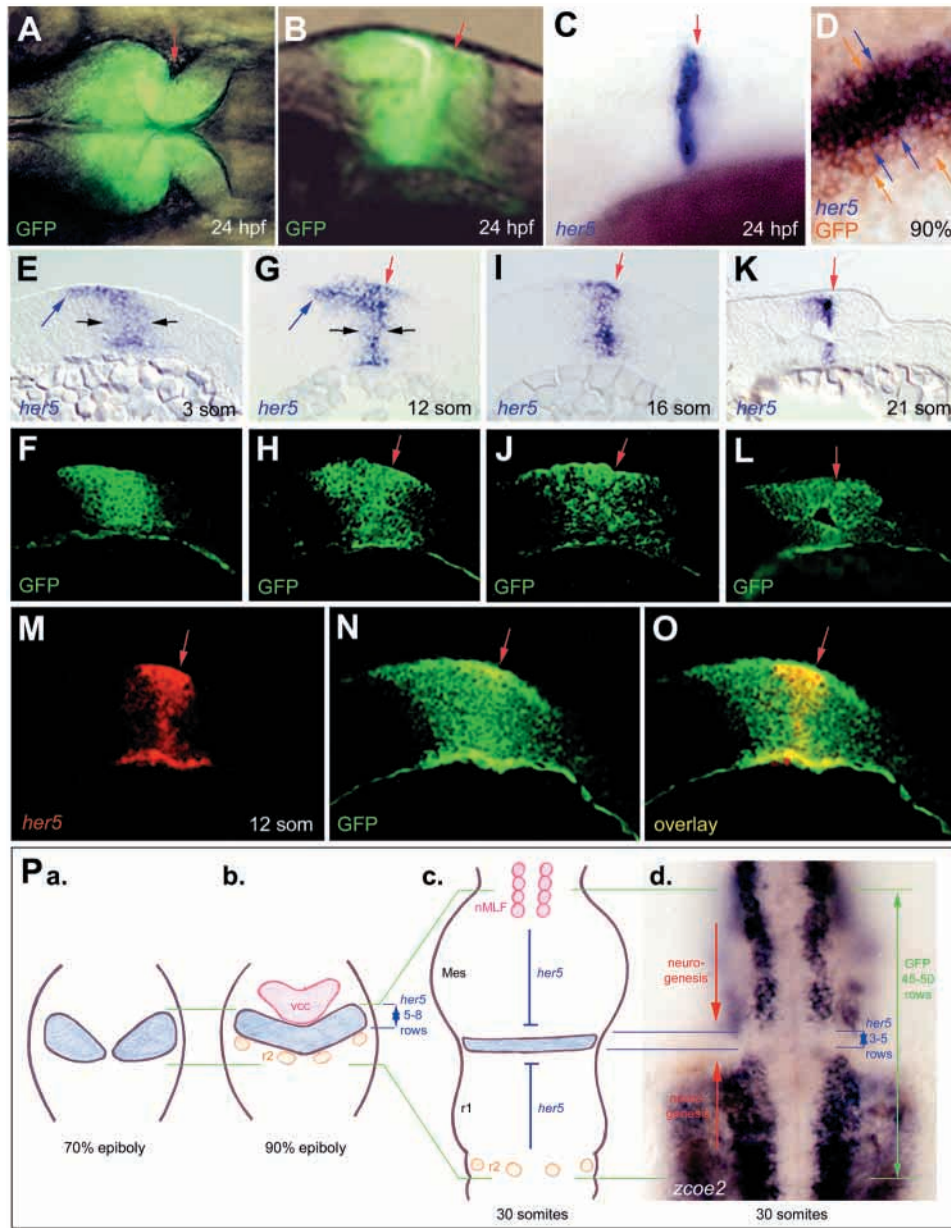
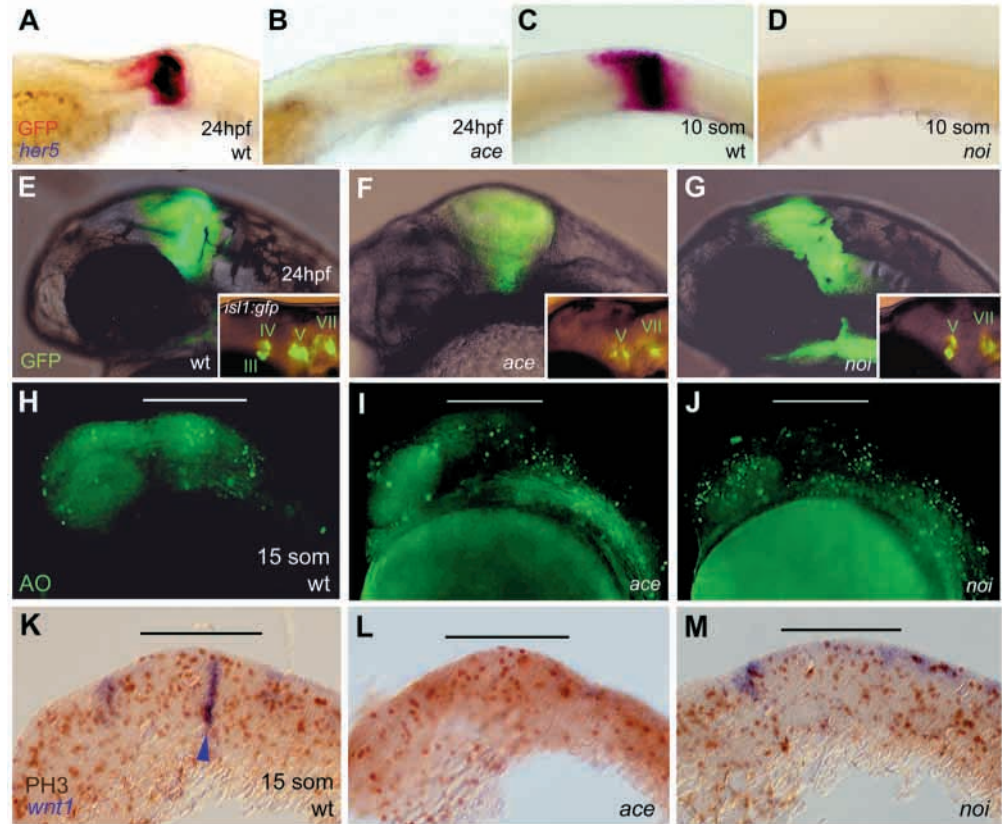


Fig. 6. Dynamic regulation of *her5* expression within the MH domain. (A-O) Comparison of *her5* expression (revealed by in situ hybridisation, blue staining in C-E,G,I,K, red staining in M,O) and GFP protein distribution (direct visualization under fluorescence microscopy, green in A,B; or revealed by anti-GFP immunocytochemistry, brown staining in D or green staining in F,H,J,L,N,O) in *her5PAC:egfp* embryos at the stages indicated. (A-D) Whole-mount views (A, dorsal, anterior leftwards; B,C, lateral, anterior leftwards; D, dorsal view of a hemi-neural plate, anterior upwards); E-O are sagittal sections, all views focus on the MH domain and are oriented anterior towards the left. The MHB is indicated by a red arrow at all stages where it is morphologically visible. (E-L) Bright field (top panels) and fluorescent (bottom panels) views of the same sections; M-O are red, green or double fluorescent views of the same section. Note the dramatic difference in the extent of *her5* transcripts (C) and GFP protein (A,B) along the AP axis at 24 hpf. Because *egfp* transcription faithfully reproduces *her5* expression in *her5PAC:egfp* embryos (Fig. 3), whereas GFP protein is stable, this demonstrates that *her5* expression is lost from progeny cells over time. This process is progressive (D-L) and sequential: it involves first a restriction of *her5* expression in the posterior aspect of the MH domain (blue and brown arrows indicate the limits of *her5* RNA and GFP protein staining, respectively, in D; blue dots indicate the posterior limit of *her5* transcription. Note that the two limits coincide anteriorly but differ by one or two cell rows posteriorly). At three somites, *her5* restriction begins in ventral and lateral aspects of the mesencephalon (black arrows in E,G), and continues after 16 somites (I) along the dorsal midline (blue arrows in E,G indicate maintained dorsal expression of *her5* prior to that stage). Note that in M-O, the final *her5* expression domain is located in the center of the GFP-positive territory, demonstrating that *her5* expression gets restricted in a converging manner towards the MHB. (P) Resulting model for the regulation of *her5* expression and the progression of neurogenesis between 70% epiboly (a), 90% epiboly (b) and 30 somites (c,d) in the MH domain [combined from the present data and data from Geling et al. (Geling et al., 2003)]. *her5* expression at 70% epiboly (blue), traced using GFP protein in *her5PAC:egfp* embryos, is the entire MH anlage (green lines and labeling, 45-50 cell rows at 30 somites). Between 70 and 90% epiboly (b), *her5* expression is lost from progeny cells posteriorly (compare green lines and blue). At 90% epiboly, *her5* expression is adjacent to the first anterior neurogenesis sites: the ventrocaudal cluster (vcc, pink, precursor of the nucleus of the medial longitudinal fascicle, nMLF) and future motor and sensory neurons of r2 (orange) (see Geling et al., 2003). At 30 somites (c), *her5* expression has been dramatically lost upon cell divisions and is restricted to three to five cell rows at the MHB. Correlatively (d), neurogenesis (revealed by *zco2* expression) (Bally-Cuif et al., 1998), still adjacent and non-overlapping with *her5* expression (compared c with d), progressed towards the MHB (red arrows) (embryo with the same orientation as in c, focus on the basal plate).

normal complement of MH precursors is present in the mutants at least until the 15-somite stage. The expression of MHB markers (Brand et al., 1996; Lun and Brand, 1998; Reifers et al., 1998), however, and of basal MH derivatives such as the III and IV cranial nerves (Fig. 7E-G, insets), is absent. Together, these results suggest that MH precursors remained in

place but, at least in part, display alternative identities in the mutants. We used the co-detection of GFP protein and diagnostic molecular markers expression on single sections to verify this hypothesis. We demonstrate below that MH progeny cells display aberrant specification in *noi* and *ace* as early as at 15 somites, when, as described above, the survival,

Fig. 7. MH precursors are maintained in *ace* and *noi* mutants. (A–D) Double in situ hybridisation for *egfp* (red) and *her5* (blue) in *her5PAC:egfp* transgenic wild-type, *ace* and *noi* siblings at the stages indicated demonstrates that *egfp* transcription also reproduces *her5* expression in *ace* and *noi*, and is downregulated following a correct schedule during the MH maintenance phase. (E–G) Live observation of *her5PAC:egfp* transgenic wild-type, *ace* and *noi* siblings under fluorescence microscopy at 24 hpf reveals that most descendants of early *her5*-positive cells (positive for GFP protein, green) are maintained, although MHB identities, such as cranial motoneurons III and IV (revealed using the *isl1:gfp* transgene, insets) (Higashijima et al., 2000) are missing. (H–M) Analyses of apoptosis (H–J, Acridine Orange staining) and cell division (K–M, anti-phosphohistone H₃ immunocytochemistry, brown staining) demonstrate that the pattern of cell death and proliferation are comparable in the MH area (bar) in wild-type, *ace* and *noi* siblings at least until the 15-somite stage. Embryos in K–M are double stained for *wnt1* expression, which is strongly downregulated in *ace* and absent in *noi* at that stage (blue staining, arrowheads).



proliferation and migration of MH cells do not show signs of perturbation.

The anterior limit of GFP protein abuts at all stages the caudal border of *pax6.1* expression (Fig. 8A,C,E,G), a marker for the posterior diencephalic alar plate. Strikingly, however, *ace* mutants showed a significant overlap between these two patterns at the 30-somite stage (Fig. 8B,B'), where a large number of cells in the anterior part of the GFP-positive territory co-expressed *pax6.1*. A transient overlap in the expression of Pax6 and En has been documented in chicken (Matsunaga et al., 2000a), suggesting that the co-expression (GFP and *pax6.1* in *ace* might result from a failure to downregulate *pax6.1* in anterior MH precursors. However, in a precise comparison of *pax6.1* and GFP, as well as of *pax6.1* and Eng proteins expression in zebrafish, we failed to observe an overlap of these markers at any stage (Fig. 8E,G and data not shown). Thus, the co-expression of GFP and *pax6.1* in *ace* rather reflects aberrant *pax6.1* transcription in MH precursors. A time-course experiment further revealed that GFP-positive cells in *ace* express a *pax6.1*-positive identity at least as early as the 15-somite stages (Fig. 8, compare F,F' with E and H,H' with G). In striking contrast to these findings, a distinct *pax6.1*/GFP border was maintained in *noi*, although *pax6.1* expression appeared extended posteriorly compared with its wild-type pattern (compare Fig. 8C with 8D).

Diencephalic cells are also characterized by the expression of *fgfr3* (Fig. 8I). In wild-type transgenic embryos, the GFP-positive territory abuts the caudal border of *fgfr3* expression

(Fig. 8I, green arrowheads), which thus shares a common posterior limit with *pax6.1*. As reported previously, we found that *fgfr3* expression extends ectopically towards caudal in *ace* and *noi* (Sleptsova-Friedrich et al., 2002). Double labeling of transgenic mutants reveals, in addition, that GFP and *fgfr3* expression overlap extensively in *noi*, where all GFP-positive cells co-express *fgfr3* (Fig. 8K), at least from the 15-somite stage onwards (Fig. 8L). By contrast, the *fgfr3*/GFP border is maintained in the *ace* alar plate. Both markers overlap in the *ace* basal plate (Fig. 8J), however, further documenting the differential plasticity of basal and alar MH precursors (see Lun and Brand, 1998; Reifers et al., 1998; Sleptsova-Friedrich et al., 2002).

Metencephalic derivatives such as the cerebellum fail to develop in both *ace* and *noi*, but the fate of metencephalic progenitors is unknown. To address this question, we relied on the expression of *otx2*, a marker of the fore- and midbrain, but not hindbrain territories. In *ace* mutants, we found that the posterior limit of *otx2* expression precisely coincided with the posterior border of GFP protein distribution (Fig. 8N). Because no extensive cell death was observed in the mutants (Reifers et al., 1998) (Fig. 7I and data not shown), this result highlights that metencephalic precursors display an *otx2*-positive identity in the absence of Fgf8 function. By contrast, in *noi* mutants, the caudal border of *otx2* expression appeared to be located half way through the GFP-positive domain, in a manner reminiscent of the wild-type situation (Fig. 8M,O). Thus, some AP distinctions related to ante- and post-MHB differences are

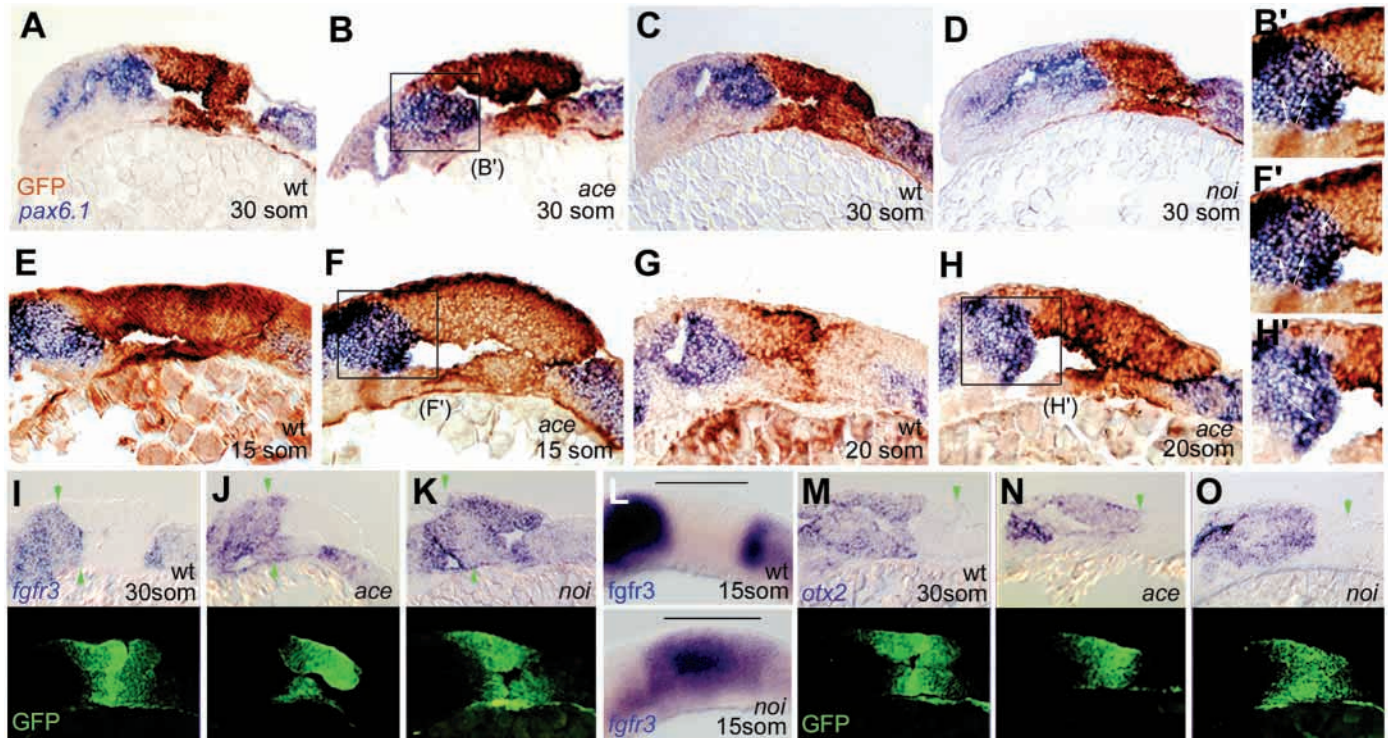


Fig. 8. MH precursors display altered molecular identities in *ace* and *noi* mutants. (A–H') Comparison of GFP protein (anti-GFP immunocytochemistry, brown staining) and *pax6.1* RNA (ISH, blue staining) at the stages indicated in sagittal sections of *her5PAC:egfp* transgenic wild-type (A,C,E,G), *ace* (B,B',F,F',H,H') and *noi* (D) embryos. B', F' and H' are magnifications of the areas boxed in B, F and H. Note that GFP protein and *pax6.1* expression are never co-expressed anteriorly in wild type (A,C,E,G) and *noi* (D), while extensive overlap between the two stainings is present in *ace* at the 15-, 20- and 30-somite stages (F',H',B'). (I–K,M–O) Comparison of GFP protein (anti-GFP immunocytochemistry, bottom panels, green staining) and *fgfr3* (I–K) or *otx2* (M–O) RNAs (in situ hybridisation, top panels, blue staining) at the stages indicated in *her5PAC:egfp* transgenic wild-type (I,M), *ace* (J,N) and *noi* (K,O) embryos. Top and bottom panels are bright-field and fluorescence views, respectively, of the same sagittal sections. Green arrowheads on the bright-field pictures point to the limits of GFP protein distribution. Note in *ace* that anterior GFP-positive cells do not co-express *fgfr3* (J, compare with I), and that posterior MH cells are all *otx2*-positive (N, compare with M). By contrast, in *noi*, all the descendants of MH precursors express *fgfr3* (K) but an *otx2*-negative territory is maintained within the caudal GFP-positive population (O). (L) Expression of *fgfr3* revealed by whole-mount in situ hybridisation shows that MH precursors in *noi* are *fgfr3*-positive already at the 15-somite stage (bar, bottom panel, compare with wild-type sibling, top panel).

maintained by the descendants of MH progenitors in *noi*. Posterior GFP-positive, *otx2*-negative cells also express *fgfr3* at high levels (Fig. 8K), suggesting that they are of posterior r1 or r2 identity. However, because of the dynamic posterior limit of GFP protein distribution in the hindbrain (Fig. 4K–Q), it was not possible to follow these cells.

Together, our findings demonstrate that MH precursors display aberrant spatial identities in *ace* and *noi*, in a manner that strikingly depends on the mutant context. An interpretative summary of our results is presented in Fig. 9.

DISCUSSION

In this article, we construct transgenic tools to trace precisely the progeny of *her5*-expressing cells during zebrafish embryogenesis, and we use these tools in a detailed analysis of the dynamics of MH development. Our tracing of *her5* progeny in wild-type and mutants leads to three important conclusions. First, we demonstrate that *her5* expression at its onset defines the MH anlage, making *her5* the first marker of the MH territory. Second, we show that *her5* expression is

progressively lost upon cell division in a spatially controlled manner towards the MHB. Because *Her5* activity negatively defines neurogenesis sites (Geling et al., 2003), this result implies that MH neurogenesis is dynamically regulated and progresses towards the MHB over time. Finally, we demonstrate that MH precursors are mostly maintained but harbor alternative identities in *noi* and *ace*, and we show that these identities depend on the mutant context. Together, our findings provide models for the dynamics of MH neurogenesis and maintenance, and directly determine *pax2.1* and *fgf8* mutant gene activities for their effect on cell identity choices.

Regulatory elements controlling *her5* expression

During embryogenesis, *her5* expression follows at least three distinct phases: it is first transcribed in a subset of endodermal precursors, then induced and maintained within the presumptive MH. In addition, each phase is subject to dynamic regulation, as endodermal expression is transient (Bally-Cuif et al., 2000) and MH expression is drastically downregulated over time (this paper). Because the *her5* enhancer had not been characterized and *her5* expression is complex, we chose the ET-cloning in vitro recombination technology (Muyrers et al.,

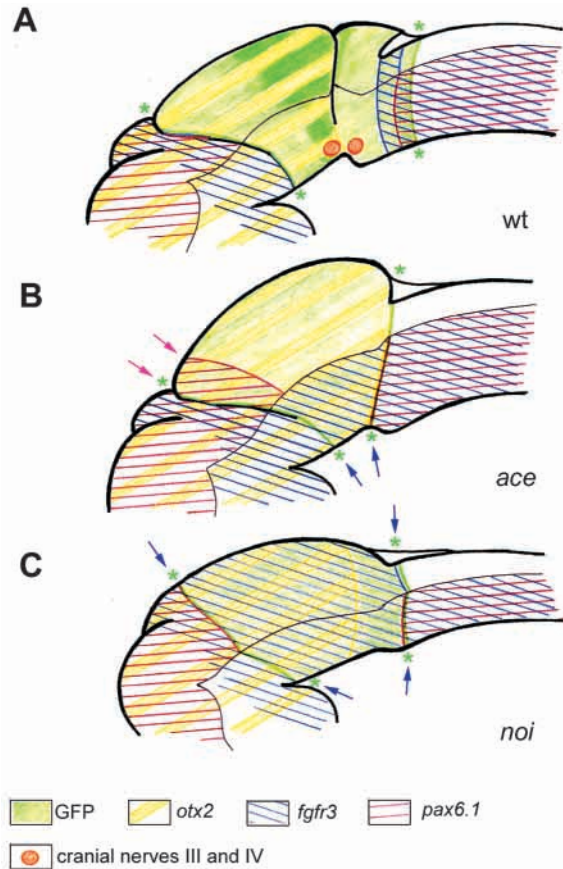


Fig. 9. Schematic representation of the fate of MH precursor cells (green, territory delimited by the green stars) in wild-type embryos (A) or in the absence of Fgf8 (B) or Pax2.1 (C) activities (interpreted from Fig. 8, and data not shown). In each drawing, the thin horizontal black line delimits the alar/basal boundary; gene expressions are color coded. Pink arrows delimit the population of anterior MH cells that acquires a *pax6.1*-positive identity in *ace* and blue arrows point to the extension of *fgfr3* expression in *noi*. Note the striking differences in the alternative identities taken by MH precursors depending on the mutant context.

2000; Muylers et al., 1999; Zhang et al., 1998) to build transgenic lines where *gfp* expression is driven by the complete set of *her5* regulatory elements. Precise analysis of *her5PAC:egfp* embryos reveals that our lines indeed fully recapitulate the phases and dynamics of in vivo *her5* expression. Our results confirm the power of artificial chromosome transgenesis in zebrafish to decipher the complexity of developmental gene regulation in vivo.

All early MH markers studied to date, including zebrafish *her5*, *pax2.1*, *eng2*, *fgf8* and *wnt1*, follow a bi-phasic mode of regulation: their expression is induced at late gastrulation, probably by independent pathways, and maintained after the five-somite stage in a mutually interdependent process (Lun and Brand, 1998; Reifers et al., 1998; Scholpp and Brand, 2001). These phases correspond to distinct regulatory elements on the promoters of zebrafish *pax2.1* (Picker et al., 2002), mouse *Pax2* (Pfeffer et al., 2002; Rowitch et al., 1999) and mouse *En2* (Li Song and Joyner, 2000; Song et al., 1996). Our deletion analysis (Fig. 2 and data not shown) failed to

dissociate initiation and maintenance elements within the *her5* enhancer, suggesting that they are closely linked and/or overlapping at the *her5* locus. The 'maintenance' elements of mouse *En2* depend upon Pax2/5/8 binding sites (Li Song and Joyner, 2000; Song et al., 1996); those of mouse *Pax2* are at least targets for auto- or crossregulation by Pax2/5/8 proteins (Pfeffer et al., 2002). *her5* expression is dependent upon the presence of Pax2.1 at somitogenesis (Lun and Brand, 1998; Reifers et al., 1998); however, analysis of the *her5* enhancer sequence failed to reveal binding sites for this maintenance factor (A.T. and L.B.-C., unpublished). In addition, we showed previously that *her5* expression was not subject to autoregulation (Geling et al., 2003). Maintenance of *her5* expression at somitogenesis thus likely involves relay factors that have yet to be identified.

A restricted subset of players involved in MH induction has been identified: the Oct-like transcription factor Spiel-ohne-Grenzen (Spg)/Pou2 (Belting et al., 2001; Burgess et al., 2002) and the Btd/Sp1-like zinc finger protein Bts1 (Tallafuss et al., 2001). Accordingly, Oct- and Sp1-binding sites are found on the early-acting enhancer of mouse *Pax2*, and at least the Oct sites are required for enhancer activity (Pfeffer et al., 2002). Similarly, we found that several Oct and Sp sites are present on the *her5* MH enhancer (A.T. and L.B.-C., unpublished). The requirement for these specific sites for *her5* induction remains to be directly demonstrated; suggestively, however, endogenous *her5* expression (Reim and Brand, 2002) and *her5PAC*-driven *gfp* expression (A.T. and L.B.-C., not shown) followed the same decreased and delayed induction in *spg/pou2* mutants compared with wild-type siblings. Factors restricting *her5* expression to the MH anlage also remain crucial components of the MH induction process to be identified. Some of these likely bind the distal region of the *her5* enhancer, as proximal domains drove unrestricted reporter expression to the anterior brain in our transgenic assays (Fig. 2F,G).

***her5* expression is the earliest marker of MH fate**

GFP protein distribution (Fig. 4) and direct mapping of the anterior and posterior extremities of the earliest *her5*-positive domain within the neural plate (Fig. 5) position the early anterior *her5* expression border to the di-mesencephalic boundary, while the posterior border of *her5* expression is more dynamic and expands, at early stages, a minor contribution into r3 and r4. GFP-positive cells found in r3 and r4 might be accounted for by a transient overlap of *her5* expression with the r3/r4 anlage at gastrulation. However, at this stage, *her5* is not co-expressed with *hoxa-1* (later renamed *hoxb1b*) (A.T. and L.B.-C., unpublished), interpreted to extend to the r3/r4 boundary (Koshida et al., 1998). Thus, alternatively, the contribution of GFP-positive cells to r3 and r4 might result from the migration of metencephalic cells towards caudal, followed by an acquisition of posterior identities (as revealed, for example, by their expression of *krox20*) (Fig. 4N). Such migration has been documented in the chicken embryo at a later stage (Marin and Puelles, 1995). We cannot formerly exclude either possibility at this point.

Outside this marginal contribution to posterior rhombomeres, the large majority of GFP-positive cells is confined to mesencephalic (midbrain, isthmus) and metencephalic (r1, r2) derivatives. GFP expression

encompasses the entire extent of the MH domain, and displays a ubiquitous distribution within this domain. Thus, our results identify *her5* expression at its onset as a comprehensive marker of MH precursors. *her5* expression at 90% epiboly was fate mapped to the midbrain only (M ller et al., 1996), an observation in agreement with the immediate restriction of *her5* expression from posterior cells between 70% and 90% epiboly (Fig. 6D), and with the identification of these posterior cells as metencephalic precursors (Fig. 5D,E). The MH domain is generally considered as an entity because its different sub-territories develop in a concerted fashion (in direct or indirect response to IsO activity), and because it is globally characterized by the expression of molecular markers (such as *En2*) at somitogenesis stages (Martinez, 2001; Rhinn and Brand, 2001; Wurst and Bally-Cuif, 2001). Our results add support to these ideas by providing the first direct molecular evidence for the definition of a MH prodomain ('pro-MH') at early developmental stages. Furthermore, they show that the AP distribution of precursors within this pro-domain displays some degree of spatial coherence as it prefigures the organization of the later MH.

The earliest *her5* expression domain defines pro-MH cells although *Her5* function itself does not control the acquisition or maintenance of MH identity (Geling et al., 2003). It is thus likely that (as yet unidentified) MH identity factors display an expression profile similar to *her5* at gastrulation. These factors might be rapidly relayed in time by *Pax2.1* and/or *Eng2/3*.

Dynamic regulation of *her5* expression and the spatiotemporal progression of MH neurogenesis

An important demonstration of our study is the highly dynamic regulation of *her5* expression over time. Indeed *her5* expression restricts from a domain covering the entire MH anlage at 70% epiboly to a few cell rows at the MHB at late somitogenesis (Fig. 6). We believe that this restriction is functionally relevant, as the spatiotemporal distribution of the *Her5* protein is likely to follow very closely that of *her5* mRNA. Indeed, *her5* mRNA is always found directly adjacent to sites undergoing neurogenesis (Geling et al., 2003) (Fig. 6P), and *Her5* protein potentially inhibits neurogenesis (Geling et al., 2003).

Between 70% epiboly and late somitogenesis, the total number of *her5*-expressing cells remains roughly unchanged; by contrast, the number of MH cells greatly increases. This observation demonstrates that *her5* expression is progressively lost upon cell divisions in a converging manner from anterior and posterior towards the MHB. Whether this progressive downregulation follows an asymmetrical mode of cell division, where *her5* expression is maintained in every other progeny cell at each cellular generation, or rather results from the progression of a maturation gradient within the MH in a manner unrelated to cell cycle events, remains to be determined. This will require the tracing of single GFP-positive cells.

Our results correlatively demonstrate that primary neurogenesis converges from anterior and posterior towards the MHB over time (Fig. 5P), and suggest that neurogenesis progression is permitted by the dynamic downregulation of *her5* expression (Geling et al., 2003). Along the DV axis of the neural tube, the combinatorial differentiation-promoting and differentiation-inhibiting activities of *Shh* and *Wnt* signaling,

respectively, has been proposed to account for the global ventral-to-dorsal progression of neuronal maturation (Megason and McMahon, 2002). *Her5* might be regarded as a counterpart to *Shh* and *Wnt* along DV, which controls the spatial order of neurogenesis progression along AP within the MH domain.

Within the MH basal plate, neuronal identity varies according to, and has been postulated to depend on, the position of the population considered relative to the MHB (Agarwala and Ragsdale, 2002; Broccoli et al., 1999; Wassarman et al., 1997). For example, nMLF reticulospinal neurons lie at the anterior border of the mesencephalon, while motoneurons (of cranial nerves III and IV) are found adjacent to the MHB. Our results on *her5* and neurogenesis dynamics also imply that these neurons are generated at different times, the former being an early and the latter a late neuronal type. Along this line, the combined action of the two E(spl)-like factors *Hes1* and *Hes3* is required for IZ maintenance in the E10.5 mouse embryo (Hirata et al., 2001), and premature neurogenesis at the MHB in *Hes1^{-/-};Hes3^{-/-}* embryos is correlated with the loss of some but not all neuronal identities that normally develop around the MHB after E10.5 (Hirata et al., 2001). Whether the primary determinant of neuronal identity is the AP location of the different populations, or rather is the timing of their engagement into the differentiation process, primarily controlled by *her5* restriction, becomes an important aspect of MH development to address in future studies.

Plasticity of MH precursors and reinforcement of MH identity

A major interest of our lines is to permit the direct tracing of MH precursors in mutant or manipulated contexts. We focused here on the *noi* and *ace* mutants, where the fate of pro-MH cells is unknown (Lun and Brand, 1998; Reifers et al., 1998). Our tracings first demonstrate that, in these mutants, a large proportion of these cells are maintained but partially acquire alternative AP identities. Second, they reveal dramatic differences in the final identities of MH precursors between the *noi* and *ace* contexts. These findings, discussed below, suggest models for the acquisition of MH fate in vivo, and clarify the respective roles of *Pax2.1* and *Fgf8* in this process.

As previously discussed, the expression of *her5* reveals that a pro-MH domain is identified at gastrulation stages within the neural plate. Several studies demonstrate that, at somitogenesis stages, the IsO is then necessary for the development of structures surrounding the MHB (such as the posterior tectum, isthmus and cerebellum). Thus, one likely function of the IsO is to permit or reinforce the diversification of MH identities at the center of the MH pro-domain. In addition, we directly demonstrate here that, in *noi* and *ace*, at least anterior and posterior MH precursors acquire characteristics of non-MH neighboring territories. Anteriorly, MH precursors express diencephalic markers (*pax6.1* in *ace*, *fgfr3* in *noi*). Posteriorly, in *noi*, *otx2*-negative MH precursors express *pax6.1* and *fgfr3* (Fig. 7), suggesting that r1 precursors express r2 characteristics. Thus, another function of IsO factors such as *Pax2.1* and *Fgf8* is to stabilize MH identity at the extremities of the MH pro-domain. Several mechanisms could account for this function. For example, the activity of IsO factors could (directly or not) act on cell movements to retain MH precursors away from more anterior or posterior patterning sources.

Alternatively, IsO factors could bias or stabilize anterior and posterior MH precursors in their choice(s) of cell identity, favoring the reinforcement of MH values. We favor this interpretation, because we did not detect obvious signs of ectopic cell migrations in *noi* and *ace*, where GFP-positive cells remained in a compact and homogeneous domain. IsO factors could either be in themselves instructive to impart or reinforce MH identities at the boundaries, or render pro-MH cells responsive to instructive cues at the proper time.

The stage at which this activity takes place cannot directly be inferred from our data. Gain- and loss-of-function experiments in the mouse, chick and zebrafish demonstrated an antagonism between the expression of Pax6 and En factors to delimit the di-mesencephalic border (Araki and Nakamura, 1999; Liu and Joyner, 2001; Mastick et al., 1997; Matsunaga et al., 2000b). Our time-course expression studies in *ace* however suggest that aberrant cell identity choice occurs at least as early as the 12-somite stage (see *pax6.1* at 15 somites on Fig. 8F, and data not shown). Furthermore, in *noi*, MH precursors acquire *fgfr3* expression but the *pax6.1*/GFP boundary is maintained. Therefore, in anterior cells of the MH pro-domain, we favor a model where IsO factors influence cell identity choices independently of Pax6 action, most probably at an earlier stage than the Pax6/En interplay. Because most MH markers display normal expression profiles in both mutants until the five-somite stage, impaired choices of identity in MH precursors in *noi* and *ace* might occur after that stage, in relation with a deficient MH maintenance loop. Alternatively, they might occur before the maintenance phase, when Pax2.1 and Fgf8 are broadly expressed within the MH anlage (Lun and Brand, 1998; Reifers et al., 1998). These choices might take place progressively, perhaps in a manner starting at the extremities of the pro-MH domain and converging towards the MHB, as suggested by the progressive restriction of MH markers (directly demonstrated here for *her5*) and the progression of maturation events such as neurogenesis (this paper).

In *noi*, *pax6.1* expression is extended posteriorly (this paper Fig. 6); however, this diencephalic expansion does not occur by recruiting mesencephalic precursors. It is possible that cell death (Brand et al., 1996) or lower proliferation rate at a late stage, or altered influences of midbrain cells on diencephalic development account for the observed posterior expansion of *pax6.1* expression. These results stress the importance of direct lineage tracing in the interpretation of patterning phenotypes.

Distinct functions of Fgf8 and Pax2.1 in cell identity choices of pro-MH cells

In the light of the model proposed above, our results highlight strikingly different impacts of the *noi* and *ace* backgrounds on the orientation of identity choices of MH precursors. Major differences are (1) the anterior expression of *pax6.1* in alar MH precursors in *ace* but not *noi*; (2) the acquisition of *fgfr3* expression by all alar cells in *noi*, while no alar cells express *fgfr3* in *ace*; and (3) the expression of *otx2* by posterior MH precursors in *ace*. Several (non-exclusive) interpretations can account for the differential plasticity of pro-MH cells in *ace* versus *noi*. Timing might be involved: the downregulation of MHB markers occurs generally later in *ace* (completed around the 20-somite stage) than in *noi* (completed around the 10-12-somite stage), making it possible that partial IsO activity is

maintained until a later stage in *ace* and prevents, for example, the turning-on of *fgfr3* expression by most alar MH precursors. More likely, Pax2.1 and Fgf8 exert distinct functions in the orientation of identity choices of pro-MH cells. First, *fgf8* and *pax2.1* are expressed in overlapping but non-identical domains, thus their primary and secondary target cells are probably distinct. In addition, they probably control different cellular processes. Pax2.1 appears generally required to prevent the pro-MH territory as a whole from acquiring an *fgfr3*-positive fate. In *noi*, because *otx2*-positive and -negative domains are maintained, the easiest interpretation of the *fgfr3* phenotype is an anteriorization of mesencephalic precursors and a posteriorization of metencephalic precursors. Thus, we propose that Pax2.1 activity in vivo prevents mes- and metencephalic precursors from choosing immediately neighboring, non-MH fates. These results extend previous findings in the mouse that implied Pax2 (together with Pax5) in the maintenance of MH identity or the IsO as a whole (Schwarz et al., 1997; Urbanek et al., 1997). Some MH characters are however retained in MH precursors in *noi*, like the non-expression of *pax6.1*. Because of the antagonistic effects of *noi* and *ace* on *pax6.1* and *fgfr3* expression, this is possibly due to the maintenance of early Fgf8 activity in *noi*.

By contrast, our results suggest distinct functions for Fgf8. First, Fgf8 expression prevents only the most anterior alar mesencephalic precursors from acquiring a partial diencephalic identity. Thus, we propose that Fgf8 is involved, at a distance, in the choice or reinforcement of an anterior tectal fate. Furthermore, we report that all GFP-positive cells in *ace* are *otx2* positive. As no cell death was observed, this strongly suggests that metencephalic precursors mostly choose an anterior identity in the absence of Fgf8 function. These results validate earlier interpretations of the Fgf8 mutant or gain-of-function phenotypes (Brand et al., 1996; Reifers et al., 1998; Liu et al., 1999; Martinez et al., 1999; Sato et al., 2001). Thus, another function of Fgf8 is to maintain AP distinctions within the MH pro-domain itself and permit the individualization of metencephalic versus mesencephalic identities. Ectopic expression experiments in chicken at somitogenesis stages demonstrated an antagonism between *Fgf8* and *Hoxa1* expression to delimit the r1/r2 boundary and determine r1 versus r2 identities (Irving and Mason, 2000). These results, together with ours, further suggest distinct functions of Fgf8 over time: at an early stage, Fgf8 would orient the choice of a metencephalic versus mesencephalic identity within the MH pro-domain; later, within the metencephalic anlage, it would reinforce an r1 versus an r2 character. In the mouse and chicken, Fgf8 has also been proposed to control proliferation (Lee et al., 1997). However, we could not detect gross alterations in the number of *her5* progeny cells between *ace* mutants and wild-type siblings at the stage of our analysis, suggesting that Fgf8 alone, in the zebrafish, does not initially play a major role in MH growth.

We are grateful to J. Sitz for advice on the ET-cloning strategy, to N. David for isolating the *her5* genomic PACs, and to A. Folchert and B. Tannhäuser for expert technical assistance and laboratory management. We acknowledge J. A. Campos-Ortega, V. Prince, T. Jovett, H. Takeda, S. Wilson and V. Korzh for gifts of probes, and the RZPD (Berlin) for providing the genomic PAC library. We thank all members of the L.B.-C.'s and K. Imai's laboratories for support and constructive input, J. A. Campos-Ortega for discussions, and P.

Chapouton, F. Rosa and M. Wassef for critical reading of the manuscript. Work in L.B.-C.'s laboratory is supported by a VolkswagenStiftung 'junior research group' grant and DFG grant BA2024/2-1.

REFERENCES

- Agarwala, S. and Ragsdale, C. W. (2002). A role for midbrain arcs in nucleogenesis. *Development* **129**, 5779-5788.
- Alvarado-Mallart, R.-M., Martinez, S. and Lance-Jones, C. (1990). Pluripotentiality of the 2-day old avian germinative neuroepithelium. *Dev. Biol.* **139**, 75-88.
- Araki, I. and Nakamura, H. (1999). Engrailed defines the position of dorsal di-mesencephalic boundary by repressing diencephalic fate. *Development* **126**, 5127-5135.
- Bally-Cuif, L., Dubois, L. and Vincent, A. (1998). Molecular cloning of Zco2, the zebrafish homolog of Xenopus Xco2 and mouse EBF-2, and its expression during primary neurogenesis. *Mech. Dev.* **77**, 85-90.
- Bally-Cuif, L., Goridis, C. and Santoni, M. J. (1993). The mouse NCAM gene displays a biphasic expression pattern during neural tube development. *Development* **117**, 543-552.
- Bally-Cuif, L., Goutel, C., Wassef, M., Wurst, W. and Rosa, F. (2000). Coregulation of anterior and posterior mesendodermal development by a hairy-related transcriptional repressor. *Genes Dev.* **14**, 1664-1677.
- Belting, H. G., Hauptmann, G., Meyer, D., Abdelilah-Seyfried, S., Chitnis, A., Eschbach, C., Soll, I., Thisse, C., Thisse, B., Artinger, K. B. et al. (2001). *spiel ohne grenzen/pou2* is required during establishment of the zebrafish midbrain-hindbrain boundary organizer. *Development* **128**, 4165-4176.
- Brand, M., Heisenberg, C. P., Jiang, Y. J., Beuchle, D., Lun, K., Furutani-Seiki, M., Granato, M., Haffter, P., Hammerschmidt, M., Kane, D. A. et al. (1996). Mutations in zebrafish genes affecting the formation of the boundary between midbrain and hindbrain. *Development* **123**, 179-190.
- Broccoli, V., Boncinelli, E. and Wurst, W. (1999). the caudal limit of Otx2 expression positions the isthmus organizer. *Nature* **401**, 164-168.
- Buchholz, F., Angrand, P. O. and Stewart, A. F. (1996). A simple assay to determine the functionality of Cre or FLP recombination targets in genomic manipulation constructs. *Nucl. Acids Res.* **24**, 3118-3119.
- Burgess, S., Reim, G., Chen, W., Hopkins, N. and Brand, M. (2002). The zebrafish *spiel-ohne-grenzen* (*spg*) gene encodes the POU domain protein Pou2 related to mammalian Oct4 and is essential for formation of the midbrain and hindbrain, and for pre-gastrula morphogenesis. *Development* **129**, 905-916.
- Crossley, P., Martinez, S. and Martin, G. (1996). Midbrain development induced by FGF(in the chick embryo. *Nature* **380**, 66-68.
- Dickmeis, T., Mourrain, P., Saint-Etienne, L., Fischer, N., Aanstad, P., Clark, M., Str hle, U. and Rosa, F. (2001). A crucial component of the endoderm formation pathway, CASANOVA, is encoded by a novel sox-related gene. *Genes Dev.* **15**, 1487-1492.
- Gardner, C. and Barald, K. (1991). The cellular environment controls the expression of engrailed-like proteins in the cranial neuroepithelium of quail/chick chimeric embryos. *Development* **113**, 1037-1048.
- Geling, A., Itoh, M., Tallafu , A., Chapouton, P., Tannh user, B., Kuwada, J. Y., Chitnis, A. B. and Bally-Cuif, L. (2003). bHLH transcription factor Her5 links patterning to regional inhibition of neurogenesis at the midbrain-hindbrain boundary. *Development* **130**, 1591-1604.
- Hallonet, M. and le Douarin, N. (1990). A new approach to the development of the cerebellum provided by the quail/chick marker system. *Development* **108**, 19-31.
- Hallonet, M., Teillet, M.-A. and le Douarin, N. (1993). Tracing neuroepithelial cells of the mesencephalic and metencephalic alar plates during cerebellar ontogeny in quail/chick chimeras. *Eur. J. Neurosci.* **5**, 1145-1155.
- Hauptmann, G. and Gerster, T. (1994). Two-colour whole-mount in situ hybridization to vertebrate and Drosophila embryos. *Trends Genet.* **10**, 266.
- Higashijima, S., Hotta, Y. and Okamoto, H. (2000). Visualization of cranial motor neurons in live transgenic zebrafish expressing green fluorescent protein under the control of the islet-1 promoter/enhancer. *J. Neurosci.* **20**, 206-218.
- Hirata, H., Tomita, K., Bessho, Y. and Kageyama, R. (2001). Hes1 and Hes3 regulate maintenance of the isthmus organizer and development of the mid/hindbrain. *EMBO J.* **20**, 4454-4466.
- Irving, C. and Mason, I. (2000). Signaling by Fgf8 from the isthmus patterns anterior hindbrain and establishes the anterior limit of Hox gene expression. *Development* **127**, 177-186.
- Kimmel, C. B., Ballard, W. W., Kimmel, S. R., Ullmann, B. and Schilling, T. F. (1995). Stages of embryonic development of the zebrafish. *Dev. Dyn.* **203**, 253-310.
- Koshida, S., Shinya, M., Mizuno, T., Kuroiwa, A. and Takeda, H. (1998). Initial anteroposterior pattern of the zebrafish central nervous system is determined by differential competence of the epiblast. *Development* **125**, 1957-1966.
- Kozlowski, D. J. and Weinberg, E. S. (2000). Photoactivatable (caged) fluorescein as a cell tracer for fate mapping in the zebrafish embryo. *Methods Mol. Biol.* **135**, 349-355.
- Krauss, S., Johansen, T., Korzh, V., Moens, U., Ericson, J. and Fjose, A. (1991). Zebrafish *pax(zf-a)*: a paired box-containing gene expressed in the neural tube. *EMBO J.* **10**, 3609-3619.
- Lee, S., Danielian, P., Fritzsche, B. and McMahon, A. (1997). Evidence that FGF8 signaling from the midbrain-hindbrain junction regulates growth and polarity in the developing midbrain. *Development* **124**, 659-696.
- Lekven, A. C., Buckles, G. R., Kostakis, N. and Moon, R. T. (2003). Wnt1 and wnt10b function redundantly at the zebrafish midbrain-hindbrain boundary. *Dev. Biol.* **254**, 172-187.
- Li, H. S., Yang, J. M., Jacobson, R. D., Pasko, D. and Sundin, O. (1994a). Pax-6 is first expressed in a region of ectoderm anterior to the early neural plate: implications for stepwise determination of the lens. *Dev. Biol.* **162**, 181-194.
- Li, Y., Allende, M. L., Finkelstein, R. and Weinberg, E. S. (1994b). Expression of two zebrafish orthodenticle-related genes in the embryonic brain. *Mech. Dev.* **48**, 229-244.
- Li Song, D. and Joyner, A. L. (2000). Two Pax2/5/8-binding sites in Engrailed2 are required for proper initiation of endogenous mid-hindbrain expression. *Mech. Dev.* **90**, 155-165.
- Liu, A. and Joyner, A. L. (2001). EN and GBX2 play essential roles downstream of FGF8 in patterning the mouse mid/hindbrain region. *Development* **128**, 181-191.
- Liu, A., Losos, K. and Joyner, A. L. (1999). FGF8 can activate Gbx2 and transform regions of the rostral mouse brain into a hindbrain fate. *Development* **126**, 4827-4838.
- Lun, K. and Brand, M. (1998). A series of no isthmus (*noi*) alleles of the zebrafish *pax2.1* gene reveals multiple signaling events in development of the midbrain-hindbrain boundary. *Development* **125**, 3049-3062.
- Macdonald, R., Xu, Q., Barth, K. A., Mikkola, I., Holder, N., Fjose, A., Krauss, S. and Wilson, S. W. (1995). Regulatory gene expression boundaries demarcate sites of neuronal differentiation in the embryonic zebrafish forebrain. *Neuron* **13**, 1039-1053.
- Marin, F. and Puelles, L. (1994). Patterning of the embryonic avian midbrain after experimental inversions: a polarizing activity from the isthmus. *Dev. Biol.* **163**, 19-37.
- Marin, F. and Puelles, L. (1995). Morphological fate of rhombomeres in quail/chick chimeras: a segmental analysis of hindbrain nuclei. *Eur. J. Neurosci.* **7**, 1714-1738.
- Martinez, S. (2001). The isthmus organizer and brain regionalization. *Int. J. Dev. Biol.* **45**, 367-371.
- Martinez, S. and Alvarado-Mallart, R.-M. (1989). Rostral cerebellum originates from the caudal portion of the so-called 'mesencephalic' vesicle: a study using chick/quail chimeras. *Eur. J. Neurosci.* **1**, 549-560.
- Martinez, S., Crossley, P., Cobos, I., Rubinstein, J. and Martin, G. (1999). FGF8 induces formation of an ectopic isthmus organizer and isthocerebellar development via a repressive effect on Otx2 expression. *Development* **126**, 1189-1200.
- Martinez, S., Wassef, M. and Alvarado-Mallart, R.-M. (1991). Induction of a mesencephalic phenotype in the 2-day old chick prosencephalon is preceded by the early expression of the homeobox gene En. *Neuron* **6**, 971-981.
- Mastick, G. S., Davis, N. M., Andrew, G. L. and Easter, S. S., Jr (1997). Pax-6 functions in boundary formation and axon guidance in the embryonic mouse forebrain. *Development* **124**, 1985-1997.
- Matsunaga, E., Araki, I. and Nakamura, H. (2000a). Pax6 defines the di-mesencephalic boundary by repressing En1 and Pax2. *Development* **127**, 2357-2365.
- Matsunaga, E., Araki, I. and Nakamura, H. (2000b). Pax6 defines the di-mesencephalic boundary by repressing En1 and Pax2. *Development* **127**, 2357-2365.
- Megason, S. and McMahon, A. P. (2002). A mitogen gradient of dorsal midline Wnts organize growth in the CNS. *Development* **129**, 2087-2098.

- Müller, M., v. Weizsäcker, E. and Campos-Ortega, J. A. (1996). Transcription of a zebrafish gene of the hairy-Enhancer of split family delineates the midbrain anlage in the neural plate. *Dev. Genes Evol.* **206**, 153-160.
- Muyrers, J. P., Zhang, Y. and Stewart, A. F. (2000). ET-cloning: think recombination first. *Genet. Eng.* **22**, 77-98.
- Muyrers, J. P., Zhang, Y., Testa, G. and Stewart, A. F. (1999). Rapid modification of bacterial artificial chromosomes by ET-recombination. *Nucleic Acids Res.* **27**, 1555-1557.
- Nakamura, H., Takagi, S., Toshiaki, T., Matsui, K. and Fujisawa, H. (1988). The prosencephalon has the capacity to differentiate into the optic tectum: analysis by chick-specific monoclonal antibodies in quail-chick chimeric brains. *Dev. Growth Differ.* **30**, 717-725.
- Narayanan, K., Williamson, R., Zhang, Y., Stewart, A. F. and Ioannou, P. A. (1999). Efficient and precise engineering of a 200 kb beta-globin human/bacterial artificial chromosome in *E. coli* DH10B using an inducible homologous recombination system. *Gene Ther.* **6**, 442-447.
- Oxtoby, E. and Jowett, T. (1993). Cloning of the zebrafish *krox-20* gene (*krx-20*) and its expression during hindbrain development. *Nucleic Acids Res.* **21**, 1087-1095.
- Palmgren, A. (1921). Embryological and morphological studies on the midbrain and cerebellum of vertebrates. *Acta Zool.* **2**, 1-94.
- Pfeffer, P. L., Payer, B., Reim, G., di Magliano, M. P. and Busslinger, M. (2002). The activation and maintenance of Pax2 expression at the mid-hindbrain boundary is controlled by separate enhancers. *Development* **129**, 307-318.
- Picker, A., Brennan, C., Reifers, F., Clarke, J. D., Holder, N. and Brand, M. (1999). Requirement for the zebrafish mid-hindbrain boundary in midbrain polarisation, mapping and confinement of the retinotectal projection. *Development* **126**, 2967-2978.
- Picker, A., Scholpp, S., Bohli, H., Takeda, H. and Brand, M. (2002). A novel positive transcriptional feedback loop in midbrain-hindbrain boundary development is revealed through analysis of the zebrafish *pax2.1* promoter in transgenic lines. *Development* **129**, 3227-3239.
- Prince, V. E., Moens, C. B., Kimmel, C. B. and Ho, R. K. (1998). Zebrafish *hox* genes: expression in the hindbrain region of wild-type and mutants of the segmentation gene, *valentino*. *Development* **125**, 393-406.
- Reifers, F., Bohli, H., Walsh, E. C., Crossley, P. H., Stainier, D. Y. and Brand, M. (1998). *Fgf8* is mutated in zebrafish acerebellar (*ace*) mutants and is required for maintenance of midbrain-hindbrain boundary development and somitogenesis. *Development* **125**, 2381-2395.
- Reim, G. and Brand, M. (2002). *Spiel-ohne-grenzen/pou2* mediates regional competence to respond to *Fgf8* during zebrafish early neural development. *Development* **129**, 917-933.
- Rhinn, M. and Brand, M. (2001). The midbrain-hindbrain boundary organizer. *Curr. Opin. Neurobiol.* **11**, 34-42.
- Rowitch, D. H., Kispert, A. and McMahon, A. P. (1999). Pax-2 regulatory sequences that direct transgene expression in the developing neural plate and external granule cell layer of the cerebellum. *Dev. Brain Res.* **117**, 99-108.
- Sato, T., Araki, I. and Nakamura, H. (2001). Inductive signal and tissue responsiveness defining the tectum and the cerebellum. *Development* **128**, 2461-2469.
- Scholpp, S. and Brand, M. (2001). Morpholino-induced knockdown of zebrafish *engrailed* genes *eng2* and *eng3* reveals redundant and unique functions in midbrain-hindbrain boundary development. *Genesis* **30**, 129-133.
- Schwarz, M., Alvarez-Bolado, G., Urbanek, P., Busslinger, M. and Gruss, P. (1997). Conserved biological function between Pax-2 and Pax-5 in midbrain and cerebellum development: evidence from targeted mutations. *Proc. Natl. Acad. Sci. USA* **94**, 14518-14523.
- Sleptsova-Friedrich, I., Li, Y., Emelyanov, A., Ekker, M., Korzh, V. and Ge, R. (2002). *fgfr3* and regionalization of anterior neural tube in zebrafish. *Mech. Dev.* **102**, 213-217.
- Song, D. L., Chalepakis, G., Gruss, P. and Joyner, A. L. (1996). Two Pax-binding sites are required for early embryonic brain expression of an *Engrailed-2* transgene. *Development* **122**, 627-635.
- Tallafuss, A., Wilm, T. P., Crozatier, M., Pfeffer, P., Wassef, M. and Bally-Cuif, L. (2001). The zebrafish buttonhead-like factor *Bts1* is an early regulator of *pax2.1* expression during mid-hindbrain development. *Development* **128**, 4021-4034.
- Thisse, C., Thisse, B., Schilling, T. and Postlethwait, J. (1993). Structure of the zebrafish *snail1* gene and its expression in wild-type, spadetail and no tail mutant embryos. *Development* **119**, 1203-1215.
- Urbanek, P., Fetka, I., Meisler, M. H. and Busslinger, M. (1997). Cooperation of Pax2 and Pax5 in midbrain and cerebellum development. *Proc. Natl. Acad. Sci. USA* **94**, 5703-5708.
- Vaage, S. (1969). Segmentation of the primitive neural tube in chick embryos. *Ergebn. Anat. Entwickl.-Gesch.* **41**, 1-88.
- Wassarman, K. M., Lewandoski, M., Campbell, K., Joyner, A. L., Rubenstein, J. L., Martinez, S. and Martin, G. R. (1997). Specification of the anterior hindbrain and establishment of a normal mid/hindbrain organizer is dependent on *Gbx2* gene function. *Development* **124**, 2923-2934.
- Williams, J. A. and Holder, N. (2000). Cell turnover in neuromasts of zebrafish larvae. *Hear. Res.* **143**, 171-181.
- Wingate, R. J. and Hatten, M. E. (1999). The role of the rhombic lip in avian cerebellum development. *Development* **126**, 4395-4404.
- Wullmann, M. and Knipp, S. (2000). Proliferation pattern changes in the zebrafish brain from embryonic through early postembryonic stages. *Anat. Embryol.* **202**, 385-400.
- Wurst, W. and Bally-Cuif, L. (2001). Neural plate patterning: upstream and downstream of the isthmus organizer. *Nat. Rev. Neurosci.* **2**, 99-108.
- Zhang, Y., Buchholz, F., Muyrers, J. P. and Stewart, A. F. (1998). A new logic for DNA engineering using recombination in *Escherichia coli*. *Nat. Genet.* **20**, 123-128.